Norwegian University
of Life Sciences

Master's Thesis 2018 30 ECTS

Faculty of Science and Technology
Department of Mathematical Science and Technology
Ingunn Burud, Associate Professor

Phenotyping Studies of Spring Wheat by Multispectral Image Analysis

Ole Kristian Lindahl Grindbakken

Environmental Physics and Renewable Energy
Faculty of Science and Technology

Acknowledgements

This master thesis complete my master's degree at Norwegian University of Life Sciences.

I would like to thank my supervisors Ingunn Burud and Morten Lillemo for their expert advise and encouraging support throughout this thesis. A special thanks goes to Bless A. K. Kufoalor for conducting the manual measurements used in the thesis. I would also like to thank Aleksander Hykkerud for excellent advise in programming.

I would like to thank my father Øyvind Asdal Grindbakken for proofreading and fruitful discussions and my mother Gry Marie Grindbakken for support and courage. Finally, I am grateful for the patience, love and support I have received from my wife Emilie Marie Lindahl Grindbakken.

Ole Kristian Lidahl Grindbakken
Ås, May 14th, 2018

Abstract

To meet an increasing demand for food production there is a need for faster genetic gains in Norwegian cereal breeding through more precise phenotyping. High-Throughput Phenotyping (HTP) and genomic selection through multispectral imaging and statistical analysis offer possibilities of yield gains. Several indices have been tested to indicate grain yield, such as the Normalized Differential Vegetation Index (NDVI), MERIS Terrestrial Chlorophyll Index (MTCI) and the Enhanced Vegetative Index (EVI). These indices utilize the difference in reflectivity in different spectral bands. The indices can indicate differences between healthy plants, stressed plants or non-plants.

The research revolves around 96 plots of 24 historical wheat cultivars and 602 plots of 301 younger breed lines. Both sites planted at Vollebekk research farm at Ås in Norway, laid out in an alpha-lattice split plot design. The design for the 24 historical cultivars had two levels of nitrogen (N) fertilization, 75 and 150 kg N/ha, applied at sowing. There were two replicates of wheat cultivars of each fertilization level. The set of 24 spring wheat represents the yield progress over the last 40 years in Norway.

Multispectral images were taken in the wavebands green (GRE) (550nm), red (RED) (660nm), red edge (REG) (735nm) and near-infrared (NIR) (790nm) with a Parrot Sequoia multispectral camera combined with a sunshine sensor. The spectral band images were stitched together using Pix4D software by utilizing GPS coordinates and image features. To aid stitching of the multispectral and RGB images, tie point objects were laid out in the field. Maps of vegetation indices were computed in Python, by forming linear combinations and ratios of sums and differences in the multispectral reflection. In addition,3D models and Digital Surface Models (DSM) of the area were calculated from RGB images using Pix4D, which were used to indicate plant height. All cameras and sensors were mounted on a light Unmanned Aerial Vehicle (UAV). Images were taken throughout the season of growth at regular intervals.

The time series of the vegetation indices showed peak values during the period of grain filling before declining when plants approached maturity. Values where slightly higher for wheat plots that received a higher dose of fertilization throughout the season of sampling. By combining the digital measurements with manual measurements of grain yield, kernel weight, and plant height, the statistical significance of separating cultivars is explored.

Keywords: multispectral imaging, vegetation, vegetation indices applications, precision farming, UAV

Table of Contents

List of Tables

List of Figures

Listings

Abbreviations

NDVI	=	**N**ormalized **D**ifference **V**egetation **I**ndex
MTCI	=	**M**ERIS **T**errestrial **C**hlorophyll **I**ndex
DSM	=	**D**igital **S**urface **M**odel
HTP	=	**H**igh **T**hroughput **P**henotyping
GPS	=	**G**lobal **P**osition **S**ystem
NIR	=	**N**ear **I**nfra**R**ed
REG	=	**R**ed **E**d**G**e
RGB	=	**R**ed, **G**reen, **B**lue
GUI	=	**G**raphical **U**ser **I**nterface
UAV	=	**U**nmanned **A**erial **V**ehicle
MSL	=	**M**ean **S**ea **L**evel
GY	=	**G**rain **Y**ield
TKW	=	**T**housand-**K**ernel **W**eight
HLW	=	**H**ectoLiter **W**eight
DH	=	**D**ays to **H**eading
DM	=	**D**ays to **M**aturity
PH	=	**P**lant **H**eight
MTP	=	**M**anual **T**ie **P**oint
CRP	=	**C**alibrated **R**eflectance **P**anel
PCA	=	**P**rincipal **C**omponent **A**nalasys
VI	=	**V**egetation **I**ndex
NMBU	=	Norwegian University of Life Sciences

Chapter 1

Introduction

To meet an increasing demand for food production, the Norwegian government have stated their goal to increase the national food production by 20% within 2030 (Landbruks- og matdepartementet, 2012). In the purpose of achieving the stated goal a comprehensive effort in scientific research is needed to ensure enough safe food. With cereal playing a key role as food and fodder for livestock, and world trends for total crop yields ceasing to improve, stagnating or collapsing (Ray et al., 2012), development of knowledge in crop potential and grain yield (GY) is desired.

Traditional methods for inspecting physiological traits and behavior of crops is time consuming and labor intensive. Earlier technologies for agricultural purposes aimed to ease labour intensive work, like tractors with computer vision (Rovira-Más et al., 2003) and smart, self driving tractors (CEMA aisbl - European Agricultural Machinery, 2017), enables the farmer to invest more time in surveying crops and planning of treatments. Implementing ”Big Data”-analysis can further contribute to technological progress in farming through the internet of things (Wolfert et al., 2017).

Remote sensing methods like multispectral imaging from unmanned aerial vehicles (UAV) (Haghighattalab et al., 2016; Tattaris et al., 2016; Montesinos-López et al., 2017; Bleken, 2017) provides a none destructive approach to examine cereal properties. Methods for estimating plant temperatures from infrared radiation and water concentration in plants (Peñuelas et al., 1997; PEñUELAS et al., 1993; Tattaris et al., 2016) have been examined,

as well as usage of RGB-images to estimate plant height (PH) and biomass (Bendig et al., 2014). These methods for observing crops will benefit the farmer in in-season treatment of growth, moreover providing a platform for high-throughput phenotyping (HTP) for plant breeders (Tattaris et al., 2016; Haghighattalab et al., 2016; Sankaran et al., 2015b,a; Montesinos-López et al., 2017). This allows breeders to evaluate a range of different traits for a large numbers of different cultivars in a fast and cost effective manner (Araus and Cairns, 2014). By using remote sensing and HTP methods breeders can select genotypes in earlier generations and thereby accelerate genetic gains by shortening the breeding cycle (Crossa et al., 2011).

The purpose of this thesis is to contribute to the understanding of HTP and the complexity of its methods by studying data collection from UAV. This thesis will ponder upon methods to obtain the spectral signature of cereal and furthermore explore correlations between the spectral signatures and admired traits, in order to help plant breeders in exploration of future cultivars. Two known vegetation indices will bi investigated, namely the MERIS Terrestrial Chlorophyll Index (MTCI), related to chlorophyll content (Zhang and Liu, 2014), and the Normalized Differential Vegetation Index (NDVI), first proposed by Tucker (1979) to be a mean of estimating biomass, but later shown to be related to the concentration of nitrogen and biomass (Gamon et al., 1995), to examine their relation to GY. A method for estimating plant height through a digital surface model (DSM) will be discussed. All three attributes, the two indices NDVI and MTCI, and the DSM, are produced from images acquired with an UAV, and later put together in a image-stitching software.

This thesis is a contribution to an on-going project called *vPheno* (viritual phenomics) started may 1st 2017. However, pilot studies have been conducted at NMBU from 2016 (Burud et al., 2017; Bleken, 2017). This thesis will utilize some of the same methods as Eivind Bleken showed in his thesis (Bleken, 2017), to further investigate the correlations of mentioned vegetation indices to characteristics and traits of different cultivars. For this thesis, two different test sites was examined. One site containing 301 relatively new breed lines of different cultivars and one smaller site containing 24 historical cultivars.

The key questions for this thesis to answer will be:

1. Will NDVI and MTCI measured on different times through the season correlate with GY?
    - Is there other manual measurements that will correlate with NDVI or MTCI?
2. Given correlations exists, will the correlation of NDVI and MTCI to GY differ between historical and young breed lines?
3. Will computer estimated plant height reflect manual measured plant height?

Chapter 2

Background and Theory

Before elaborating on methods to obtain the different vegetation indices and how their hypothetical correlation regarding different traits, this chapter will present a brief history on how the indices came to be, the utilization of them and the underlying theory on how the vegetation indices hypothetically relate to the traits.

2.1 Plant growth and health

The growth process of spring wheat can be described in stages. Zadoks et al. (1974) proposed a decimal code for distinguishing the different stages of growth. The Zadoks code is one of the most universally accepted systems (Simmons et al., 1995) with primary stages and sub stages, called secondary stages, presented in Table 2.1 with primary stages only. Germination, stage 0, starts as soon the seed is sowed followed by leaf development in stage 1. Stages 2, 3 and 4 recognized by elongation and further leaf development before head emerges in stage 5 and pollination in stage 6. The wheat plant is then going through grain filling and ripening the following weeks. It is denoted by Zadoks code as stages 7, 8 and 9. Through grain filling the moisture of the kernel decreases as the grain dry weight increases, going from milky to doughy, to hardened in the ripening season with maximum grain weight when moisture percentage is between 30 and 40 percent.

70 to 90 percent of the final grain yield is produced by photosynthates, products of photosynthesis, during grain filling (Simmons et al., 1995). Knowing chlorophyll is important

Table 2.1: Growth stages of spring wheat described by the Zadoks code.

Zadoks code	Growth stage
0	Germination
1	Seeding development
2	Tillering
3	Stem elongnation
4	Boot
5	Head Emergence
6	Flowering
7	Milk development
8	Dough development
9	Ripening

for photosynthesis (Mauzerall, 1976) gives incentives for studying chlorophyll content during the different stages of growth, especially the process of grain filling.

2.2 Reflection

When materials is exposed to electromagnetic radiation, the radiation is transmitted, reflected or absorbed depending on the nature of the given material. In plant leafs this is depending on the leaf surface properties, internal structure and biochemical components. Plants vary their sensitivity and absorption of electromagnetic radiation of different wavelengths. This varies with growth stage of the plant, but more importantly with the health of the plant (Peñuelas and Filella, 1998). By exploiting the difference in reflection in light, indices can be applied in order to classify vegetation from soil, moreover distinguish unhealthy plants form healthy ones.

One of the first utilization of these differences in reflectance was done by Rouse Jr et al. (1974), who applied calculations of the ratio between reflectance in near infrared (NIR) and RED from satellite images to survey areas of high vegetation density. A large variation on vegetation indices from satellite images was explored in the following years to study their correlations to biomass, water- and chlorophyll content (Tucker, 1979). In later years, use remote sensing in agriculture applications have increased (LeBoeuf, 2000). Exploration of UAV to serve as platforms in agricultural use has lead to reduced costs and

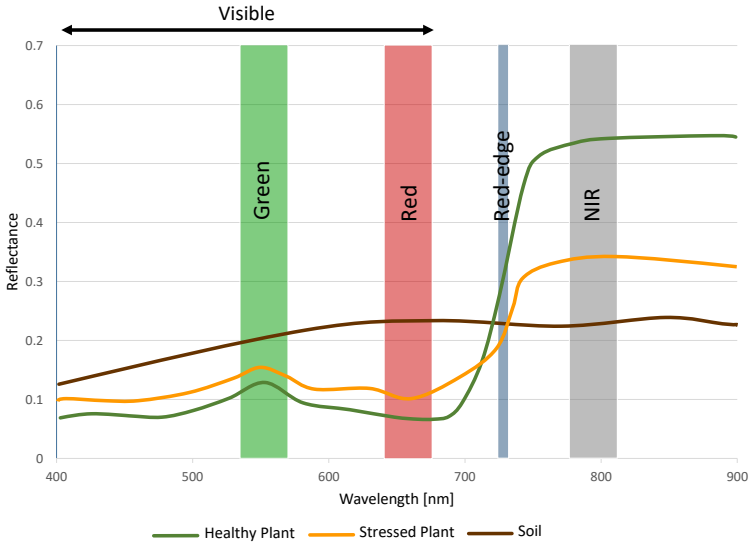

Figure 2.1: The reflectance of electromagnetic radiation from vegetation and soil.

increased resolution of images.

Perry Jr and Lautenschlager (1984) described the reflection signature of vegetation, Figure 2.1. The different amount of reflection in different spectral bands gives opportunity to form vegetation indices based on combinations of the response in the spectral bands. Figure 2.1 describes the amount of reflected radiation for healthy plants (green line), stressed plants (yellow line) and soil (brown) in the range of visible light to near infrared.

2.2.1 Normalized Difference Vegetation Index (NDVI)

The Normalized Difference Vegetation Index (NDVI) is calculated by subtracting the reflectance in the RED band from the reflectance in the NIR band. This difference is further divided on the sum of the two giving the index

$$NDVI = \frac{NIR - RED}{NIR + RED} \tag{2.1}$$

where NIR is the reflectance in the NIR band and RED is the reflectance in the RED band. The NDVI will alvays be between -1 and 1.

NDVI will have high values, near 1, for healthy vegetation, and NDVI values for soil engages positive values close to zero. In this way, NDVI will be a good feature for distinguishing between vegetation and soil.

2.2.2 MTCI

As an indicator for chlorophyll content, studies have shown that the position of the maximum slope of the curve for reflected light, called red edge (REG), in relation to the reflection of light in RED- and NIR-band, is related to the concentration of chlorophyll (Dash and Curran, 2004). Dash and Curran (2004) proposed an index for estimating chlorophyll content and through it monitoring plant health. The MERIS Terrestrial Chlorophyll Index (MTCI) was derived as

$$MTCI = \frac{NIR - REG}{REG - RED} \tag{2.2}$$

where where NIR is the reflectance in the NIR band, REG and RED is the reflectance in the REG- and the RED band respectively.

2.3 Acquiring images

2.3.1 Multispectral Cameras

There is a range of techniques for sampling multispectral images (Hagen and Kudenov, 2013). Due to different wavelength having different refraction in transparent or translucent materials, lenses and mirrors can be used to split different wavelength onto different photo sensors. Another technique is using photocells combined with filter, making the camera sensible only for a small range of wavelengths.

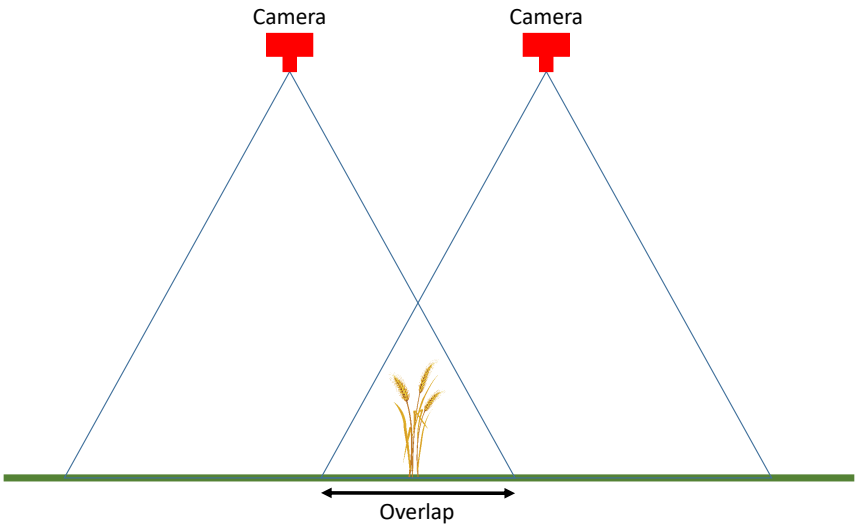

Figure 2.2: Acquiring images for photogrammetry purposes requires images to overlap.

2.3.2 Photogrammetry

To build 3D models and precise orthomosaic images, images acquired need to have high percentage of overlapping area. For sufficient accuracy, images should have at least 50-60% overlap. Both orthomosaic images and 3D models will have higher precision the more keypoints, *i.e.* points in different images recognizable from the same point on the target. Figure 2.2 is a schematic figure displaying the camera positions for two images. The target, represented by one single canopy of wheat, will have distinguishable points in both images taken. These points are used to construct a 3D mesh, which in turn are to be filled by fragments of the raw images in between the keypoints.

2.3.3 Shadowing

Image acquisition from UAVs call for homogeneous weather conditions with continuous lighting. Flying in weather with spars clouds can result in images with various illumination not corrected for. Small clouds could cast shadows upon the target without the shadow falling on the irradiance sensor (Figure 2.3). This undesirable effect is more prone to occur for the UAV flying at higher altitudes.

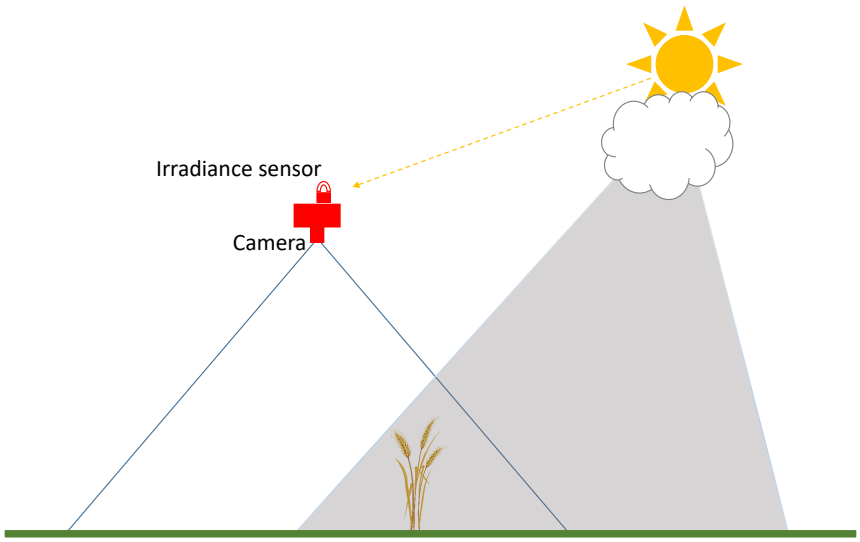

Figure 2.3: Whether with sparse cloud cover can result in images not corrected by the irradiance sensor, hence the sensor will not detect relatively small shadows.

2.4 Statistics

The plants examined in this project was planted in a *alpha lattice split plot* design, meaning that cultivars are planted in *columns*, there are six columns per *block*. There were four blocks for each level of fertilizer. And the whole set up was *replicated*. This maximizes the possibilities to study the differences between cultivars within the two levels of fertilizer. The model that was tested stated that trait was dependent on the cultivar, the level of fertilizer, and the interaction between the two. The SAS software (code given in appendix) calculated the least square mean for the specific cultivar, and the least square mean for the specific cultivar given a level of fertilizer.

PCA

To explore correlations between traits this thesis will utilize Principal component analysis (PCA) (Esbensen et al., 2002). The PCA usually use terms as *objects* and *variables* as

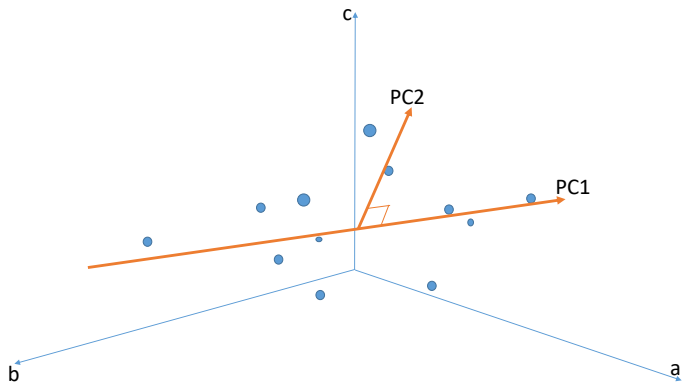

Figure 2.4: Principal components 1 and 2 (PC1, PC2) in relation to data points distributed across the abc-room.

two essential describing features of the PCA. The object is a vector with values for every measured variable. This is directly applicable to the data in this thesis. The different cultivars serves as the objects, as they have values for every trait, which will be the variables of the PCA.

The set of data points can be so large that it gets unpractical to list it as a table in order to read interesting information from it. In the nature, different variables often have something in common. Information about one variance can often give information about the other. For instance, tall people tend to have larger shoes than shorter people. In this thesis, measurements of a cultivars height and the weight of that cultivars grains will, like the shoe size of tall people, hold some information about the other one. This information is then redundant. By creating a new characteristic based on a linear combination of the two, the PCA will combine every trait in data set and eventually create a characteristic as a linear combination of all traits. The characteristic will describe maximum variation for the hole set of observations. This characteristic which maximizes variance across the data is named principal component 1 (PC1). The next principal component, PC2, lies orthogonal on PC1 and in the direction of the second largest variation in the data. A visualization of the two is given in Figure 2.4.

Every PC is constructed from a linear combination of the unit vectors. The coefficients

of in the linear combination are called *loadings*. It is the same number of coefficients for each PC as there are unit vectors. The loadings of all the PCs constructs a transformation matrix between the original space onto the space spanned by the PCs. The loadings holds information about the relationship between the PCs and the original space. It is the loadings plot that is to be examined to investigate the correlation between different traits.

Chapter 3

Method

This chapter will describe the materials for this thesis, as well as present the methods used to obtain data from the data. This includes wheat field growing conditions, gathering of image data, initial image processing and software algorithms for analysis. Furthermore describe how the acquired data was analysed.

3.1 Test site

The study site is located at Vollebekk Research Farm, Figure 3.1, near the Norwegian University of Life Sciences (NMBU) in Ås, Akershus, Norway (59°39'N 10°45'E). There is situated two experimental sites on the research farm. The two sites have different breed lines of cultivars planted. One relatively large site, with technical name 17CMLGI1, containing 301 different breed lines planted may 4th. 2017, in two replicates with the same amount of fertilizer in both replicates. The smaller site, with technical name 17BML-ROBOT1, contains 24 historical spring wheat cultivars, and was planted may 24th. 2017. The test field was split up in four segments, two for each fertilizer level of 15 kg daa^{-1} Nitrogen and 7.5 kg daa^{-1} Nitrogen. The two levels of Nitrogen fertilizer will be described in this thesis form this point on as 15 kg daa^{-1} and 8 kg daa^{-1}. Both sites was planted in a alpha lattice split plot design.

The two sites will be referred to as site A, for the larger 17CMLGI1-field, and site B for

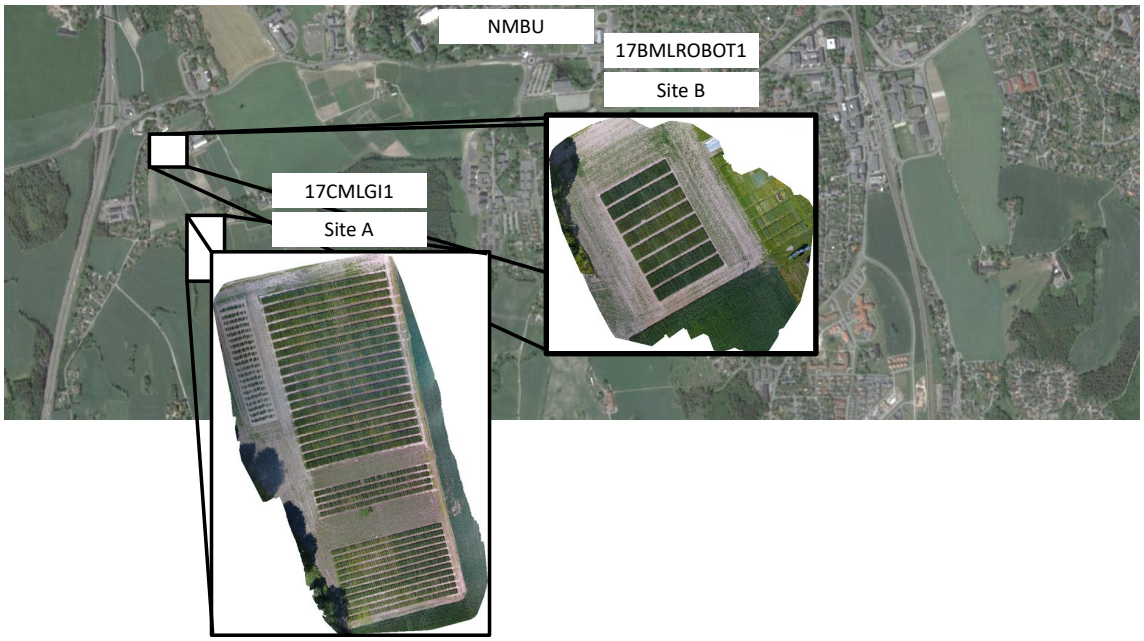

Figure 3.1: The two fields are situated at Vollebekk Research farm west of NMBU, about 35 km south of Oslo, Norway.

the smaller 17BMLROBOT1-field.

Table 3.1 shows an overview of the field design of site B. In this alpha lattice split plot design each field plot is labelled after their name, fertilizer level and replication i.e. `Name_Fertilizer-level_Replicate`. On site A (Figure 3.2), field plots is named `Name_Replicate` due to no difference in fertilizer. The statistical model tested for Site A was that trait was dependent of breed lines only.

Besides having these distinct names, every field plot is assigned a four digit identification number unique for every position in the test field. This number, ranging from 1101 to 3028 for site A, and from 1101 to 1812 in site B, contains information on what column and row a given field plot is situated. In Table 3.1 `Bastian_15_1` in the upper right corner is given the identification number of 1101, likewise `Bastian_15_2` in the lower right corner of Table 3.1 is given the number 1812. These 96 field plots makes up the set of cultivars to examine. There were planted two additional barrier columns in site B on each side to shield from environmental stress factors. On site A border columns was placed on each side, as well as two border columns in the middle.

Table 3.1: The test site B with the 96 field plots schematically shown together with their respective replication number and fertilizer level. Border field plots are not included. The schematic layout in this figure is tilted about 60°counter clockwise from its actual situation at Vollebek Research Farm.

Rep. 1				Rep. 2			
15 kg Nitrogen daa^{-1}		7.5 kg Nitrogen daa^{-1}		7.5 kg Nitrogen daa^{-1}		15 kg Nitrogen daa^{-1}	
Bastian	SW11011	Rabagast	Bjarne	Rabagast	Avle	GN11644	Arabella
GN13618	Runar	SW21074	SW11230	SW11011	Demonstrant	GN10521	Zebra
Mirakel	SW01074	GN10521	Demonstrant	Bastian	GN11644	Rabagast	SW11230
PS-1	SW11230	SW11011	Reno	Reno	Polkka	Mirakel	Runar
GN11542	Polkka	Arabella	Polkka	Runar	Arabella	SW01074	Tjalve
Arabella	Krabat	Krabat	GN11542	Tjalve	GN13618	Bjarne	Demonstrant
Avle	GN10637	Mirakel	GN10637	PS-1	SW21074	Reno	Krabat
SW21074	GN10521	Runar	Tjalve	GN10637	Krabat	Avle	GN10637
Rabagast	Zebra	GN11644	Avle	Seniorita	Zebra	PS-1	Seniorita
Seniorita	GN11644	Zebra	PS-1	GN10521	GN11542	SW11011	Polkka
Bjarne	Tjalve	Seniorita	SW01074	Bjarne	SW01074	SW21074	GN11542
Demonstrant	Reno	GN13618	Bastian	SW11230	Mirakel	GN13618	Bastian

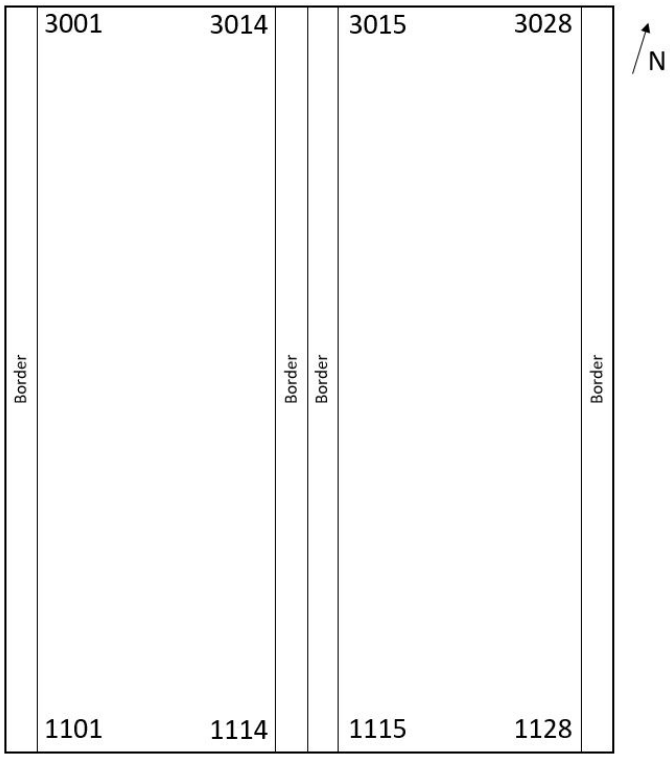

Figure 3.2: Field leyout of Site A, 17CMLGI1.

Treatment of herbicides and fungicides was applied. Manual measurements of days to heading (DH), days to maturity (DM) was carried out through the season. Plant height (PH) was measured as the cultivars reached maximum height in late season. Following maturing the test field was harvested and the two parameters; hectoliter weight (HLW) and 1000-kernel weight (TKW) was measured for site B. On site A was plant cover measured. For Both sites was grain GY measured.

3.2 Sampling

To collect images for this thesis a unmanned aerial vehicle (UAV) was used, carrying a Parrot Sequoia multispectral camera and a irradiance sensor. The camera was mounted on the UAV facing downwards, and the irradiance sensor mounted on top of the UAV. The multispectral camera had five lenses, collecting RGB-images as well as images in the spectral bands of green (550 nm), RED (660 nm), REG (735 nm) and near infrared (790 nm), resembling the specral bands precented in 2.1. The bandwidth of the image bands was 40 nm for bands green, RED and NIR, and 10 nm for REG, making the REG band the highest defined band. Images can be seen in Figure 3.3. Each of the images taken with the four spectral bands lenses had an image resolution of 1.2 mega pixels (Mpx). The RGB-camera produced images of 16 Mpx resolution. The irradiance sensor had filters for detecting the amount of incoming radiation in the mentioned four spectral bands from direct light from the sun or diffuse light from cloudy weather conditions. This allows every image to be automatically corrected for illumination differences. Once the camera and irradiance sensor was mounted and the UAV ready, the cameras were set to take images automatically at a given pace of three images every two seconds. The cameras was set to record while the UAV was still on the ground. This resulted in images taken in a range of heights as the UAV was ascending and descending.

To secure correct identification by the image processing software ground control points (GCP) where laid out in the test field. The GCPs, seen in Figure 3.4, was placed in each of the four corners of site B, and an additional GCP in the top center of site A. Additionally

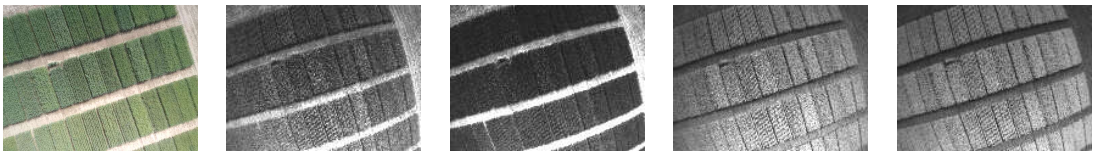

(a) (b) (c) (d) (e)

Figure 3.3: Parrot Sequoia captures one RGB image 3.3a and four images for different spectral bands green 3.3b, RED 3.3c, REG 3.3d and near infrared 3.3e

(a) (b)

Figure 3.4: Two types of ground control points (GCP) was used. One with a easily defined center depicted by a cross 3.4a, and one with a circle 3.4b.

to ease image processing, these GCPs was helpful in aligning image series throughout the season.

In an event of the irradiance sensor not function properly, a calibration target, or a Calibrated Reflectance Panel (CRP), Figure 3.5, was included in the field images. The CRP used was produced by MicaSense (MicaSense, 2018a) had a QR-code for image processing software readability and an area of known reflectance. The exact value for reflectance is confidential and are provided by MicaSense upon inquiry.

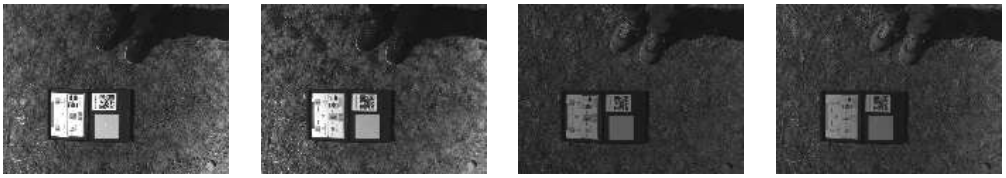

(a) (b) (c) (d)

Figure 3.5: The image calibration panel depicted in four images for different spectral bands green 3.3b, RED 3.3c, REG 3.3d and near infrared 3.3e. The uniform area next to the QR-code is the area of known reflectance.

3.3 Pix4D

The image processing software used in this thesis was Pix4D. Pix4D is a commercial image processing software specialized on solutions for surveying, construction, real estate and, for our need, agriculture. In this section, an exemplification for using Pix4D for agricultural purposes will be described by step-by-step approach.

3.3.1 Start Project

To process images from a flight into GeoTIFF images, a new project is initialized. After giving the new project a describing name, the program calls for images to process. Here is all images, like shown in Figure 3.3, for for a flight uploaded, including radiometric calibration images, Figure 3.5. Note that images from different flights may cause disturbance in triangulating images if images form the two flights do not overlap sufficiently (Pix4D, 2018b). The software will not process RGB-images and multispectral images simultaneously. They are to be processed separately.

Exif data (the metadata) for every image is read and the user is requested to remove images with invalid Exif data. In the following step, the user is allowed to inspect what Exif data is obtained from the uploaded pictures. Images taken in different heights, e.i. whilst the UAV is ascending og descending, are favourable to remove during this step.

Pix4D is already tailored for agricultural use and thus the software have templates for further processing options. Large GeoTIFF files, over 5000 pixels in any direction, will be segmented into tiles less than 5000 pixels in both directions. These tiles can be merged in Pix4D.

3.3.2 Radiometric Calibration

When loading acquired images from the field into Pix4D, images of the radiometric CRP can be included. The software is programmed to automatically detect target plates from

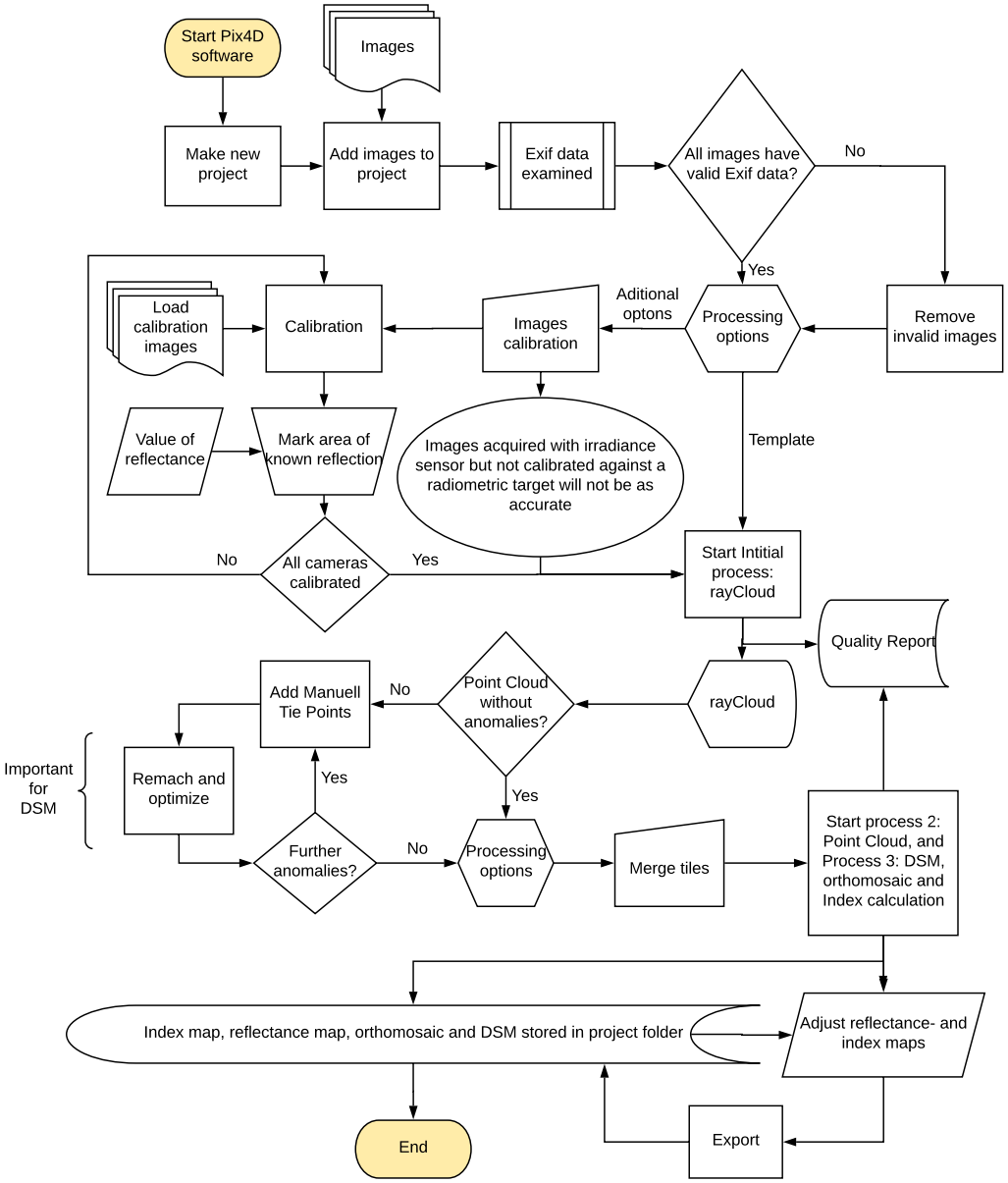

Figure 3.6: The flowchart describes the process flow of processing images in Pix4D with foresight on agricultural applications.

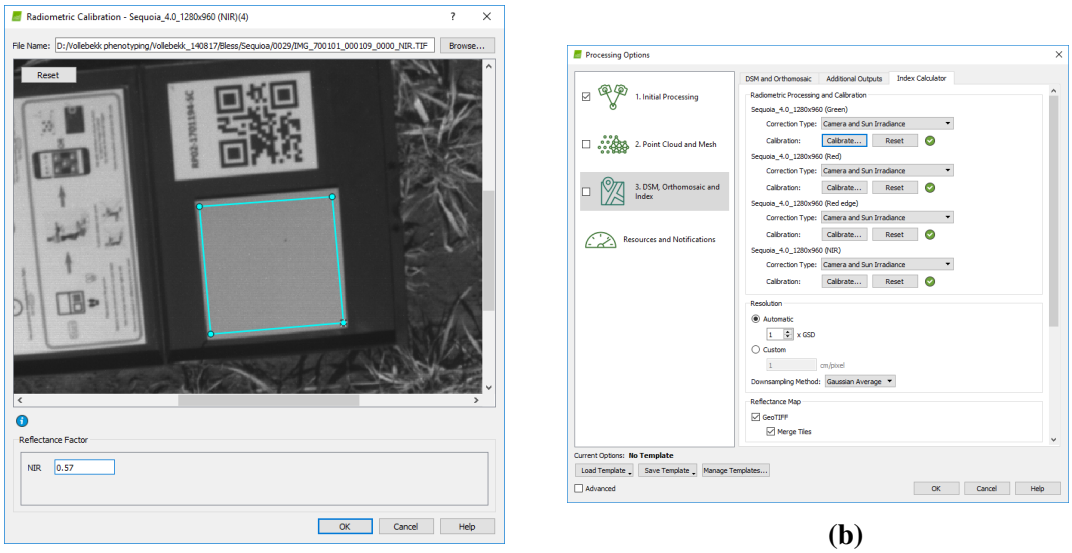

(a) **(b)**

Figure 3.7: Manuel radiometric calibration of images in Pix4D requires the user to upload a band image of the CRP 3.7a, and enter the albedo for that specific target. After repeating the process for all multispectral bands, successful calibration will be shown by green check marks 3.7b.

certain producers Pix4D (2018a). For the target used in this thesis, which was manufactured by MicaSense, automatic detection was inoperative. Successful calibration of the multispectral images required manual calibration by uploading images of the radiometric CRP in actual spectral band and by cursor clicks mark the region of known reflectance together with its value, known as *albedo* (Figure 3.7a). Successful calibration will be shown by green check marks 3.7b. Images acquired whith irradiance sensor, but processed without calibration will not be as accurate as needed for scientific research (MicaSense, 2018b; Tudor, 2018)

3.3.3 GeoTIFF Stitching

After successful calibration, the software is ready to start stitching images from the field together by triangulating points in between overlapping images. This produces a ”rayCloud”. The rayCloud gives the user options to alter and give additional input to aid rematching wrongly triangulated image points. The user can specify manual tie points (MTP), Figure 3.8. The user is requested to mark points in raw images, lower right corner of Figure 3.8, witch matches up to the same point in the field.

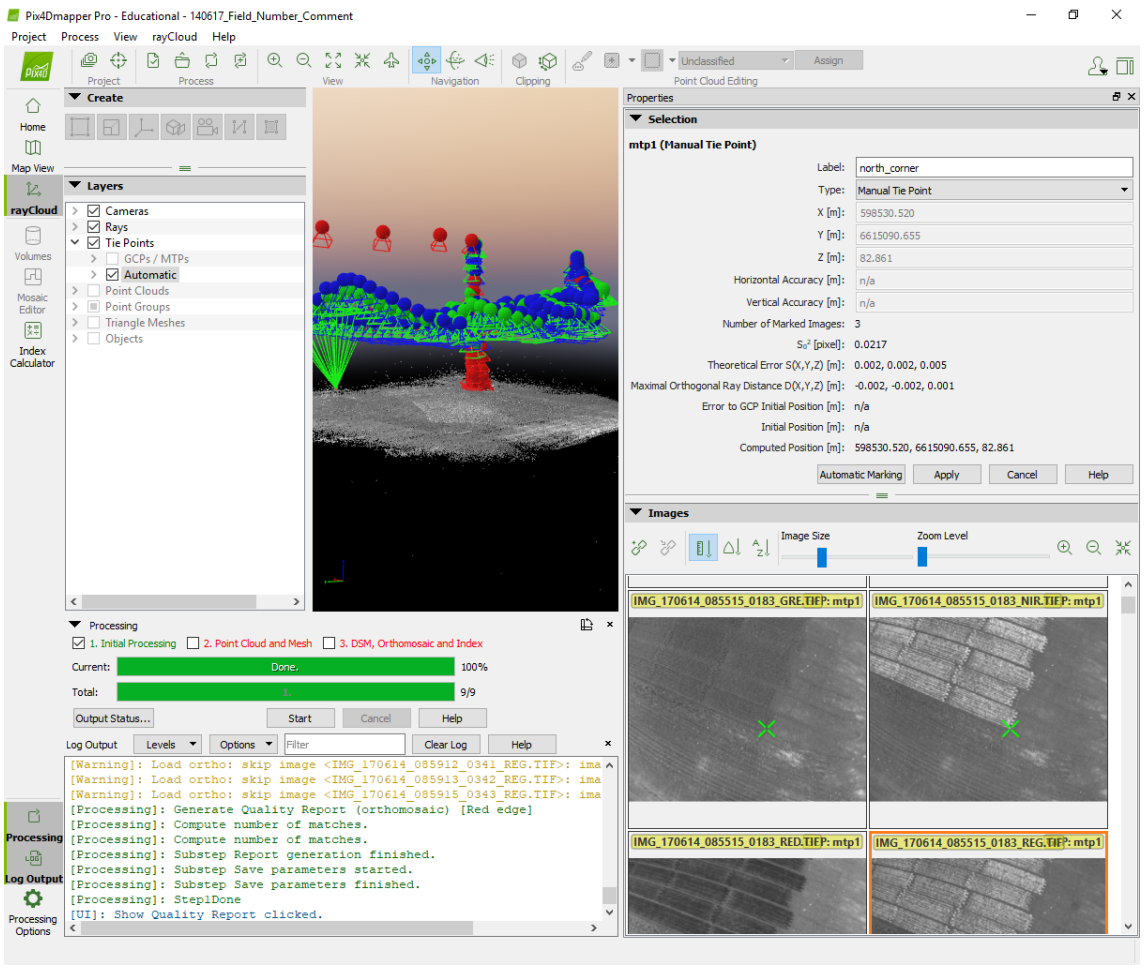

Figure 3.8: Screenshot from Pix4D during making of maunal tie points (MTP).

After marking an adequately number of MTPs, the rayCloud is updated by the user clicking ”Rematch and optimize” in the top left corner of Figure 3.8. This will present a new rayCloud. If the result is not satisfying, applying additional MTPs will help.

For larger projects where images is acquired from several flights, MTPs can be used to merge projects for better accuracy. This is done by identifying one particular MTP occurring in different flights by the same label, option seen in top right corner of Figure 3.8.

When the rayCloud is constructed free for anomalies, the groundwork for an acceptable GeoTiff image is done. The GeoTIFF, seen for the two fields are shown in Figure 3.1. The image is a constructed image of the whole area from where the UAV have captured the uploaded images. The software then produces reflectance maps for each spectral band, and index maps for defined indices. In Figure 3.9 NDVI vaulues are displayed. The user

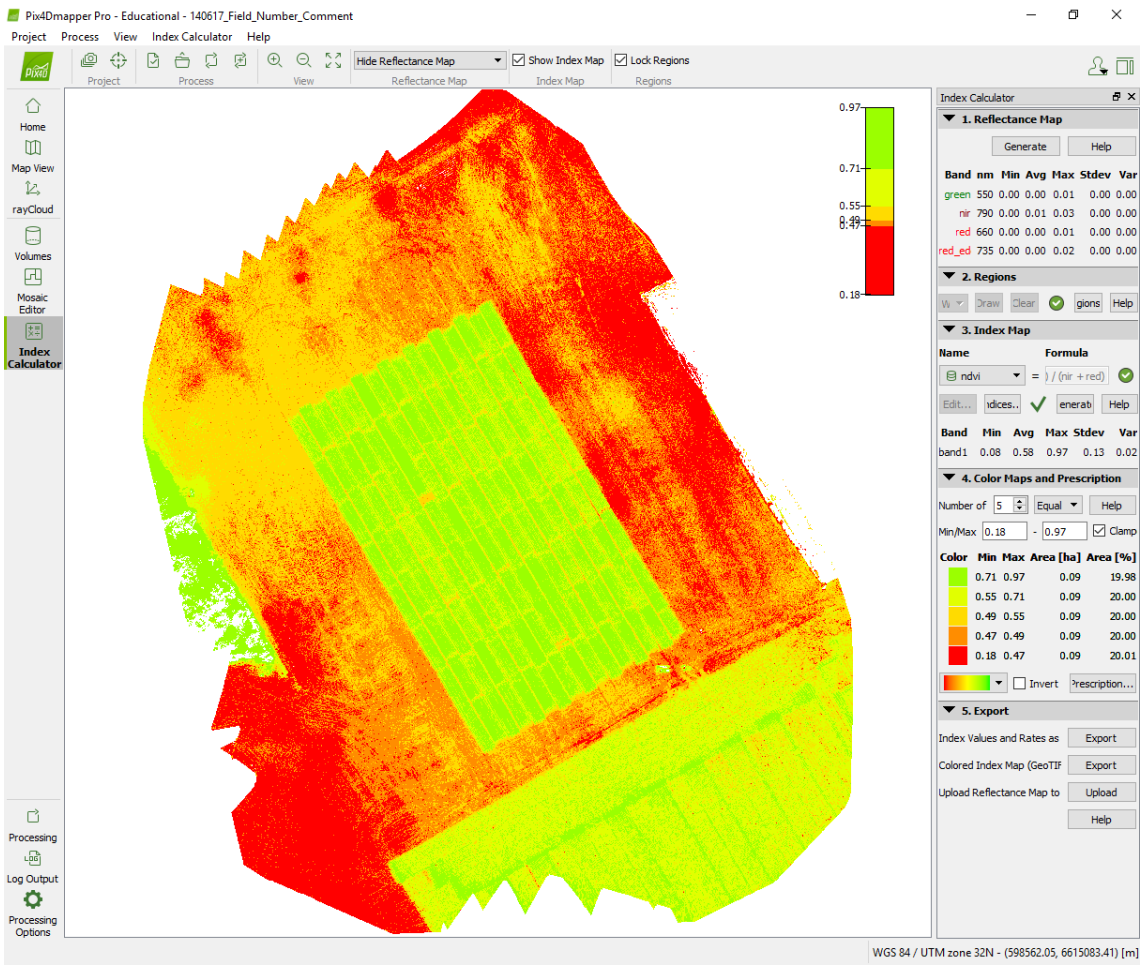

Figure 3.9: Index map in Pix4D. This index map shows NDVI values for one date used during this thesis.

is allowed to specify the range of pseudo colors used. Images can be exported to their respective project folder.

3.3.4 Digital Surface Model - DSM

Pix4D produces a visual representation of every pixels height over main see level (MSL). This image takes in consideration the global position system (GPS) data from the irradiance sensor, and triangulates the position for pixels. Images with higher resolutions will provide a more detailed DSM. For this purpose, the RGB images, which had a resolution of 16 Mpx, where used.

3.4 Data Extraction

To extract the sought data from the reflectance maps, Gunnar Lange, developed a graphical user interface (GUI) for extracting data form the different spectral band GeoTIFF images. The software reads the different spectral images as `numpy arrays` (The SciPy community, 2018a). The user of the software is requested to mark every field plot by four cursor clicks defining the area of sampled values. The sampled values is extracted from the respective spectral image and calculated by the equations 2.1 and 2.2 presented on page 7. The work flow of this software is pipelined and well described by the software user guide (Hykkerud, 2017).

3.4.1 Field Plot Segmentation

Creating an image segmentation containing one square for every field plot using the GUI of Lange's software is a time consuming and demanding process. An alternative way for producing sought mask was briefly explored in this thesis. By exploring `scipy`-package `ndimage`. An incomplete psudocode for this attempt is presented in Listing 5.8 (complete code given in appendix). Different combinations of spectral bands from both RGB images, which had greater resolution, and from multispectral images was tested. Listing 5.8 presents utilization of NDVI image because of its high contrast between vegetation and soil (Rouse Jr et al., 1974). Manual values for thresholds was determined from visual inspection of the image histogram. Further was `ndimage.binary_fill_holes` applied for making full masks.

Listing 3.1: Making a mask for data extraction.

```
img = gdal.Open('NDVI_image_name').ReadAsArray()
hist, bin_edges = np.histogram(ndvi, bins=80)
bin_centers = 0.5*(bin_edges[:-1] + bin_edges[1:])
plt.plot(bin_centers,hist)

binary_img_h = ndvi > high_threshold
binary_img_l = ndvi < low_threshold
binary_img = np.invert(binary_img_h + binary_img_l)
```

```
plt.imshow(binary_img)

fil_img = ndimage.binary_fill_holes(binary_img)
plt.imshow(fil_img)
```

3.5 Handling of Height values

3.5.1 Height data extraction

An extension to the software for extracting height values for the field plots is made during this thesis. The extension is written on a duplicate of Gunnar Lange's Python script. This allows a fast extraction of data for every field plot in the field, over longer time series.
The height values is given from the DSM as meter over mean sea level, so an conversion algorithm to present the plant height (PH) in comparable units was made. Bleken (2017) proposed a simple, yet effective method for convert DSM values into PH in his thesis. Eivind Bleken proposed to sample DSM values in between rows and columns and thus creating a regression model of the ground to subtract from the DSM values for the field plots.

In this thesis a mehtod similar to that Bleken (2017) proposed was used. Using the extension to Lange's software enables extracting values in between rows for DSM images throughout the season. The areas to serve as ground reference, shown in Figure **??**, are sampled in between rows at three points for every gap between the rows.

Python Code

The code in Listing 3.2, which is a snippet from the total code, describes the regression of ground sample values. It itterates though the eight rows making a new regression line for each row. The test field had 16 columns, included two border columns on both sides. Ground height samples was carried out just outside column one, between column eight and nine and just outside column 16. The positions across columns for ground samples is then 0.5, 8.5 and 16.5 in values of column number. The height value for sampled point in the gap north of, and south of given row is then averaged in order to estimate

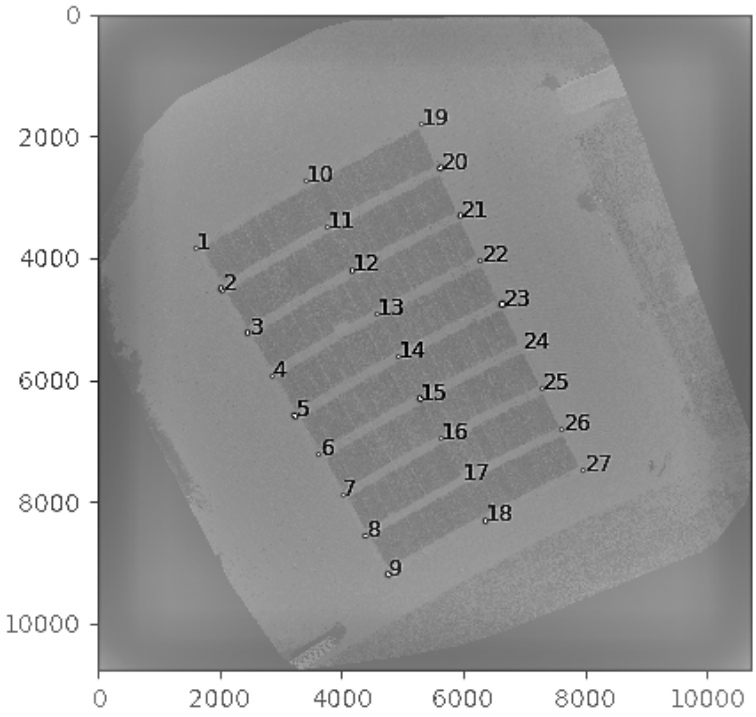

Figure 3.10: The image is a product of Lange's software. The small areas serving as ground reference for calculating PH. The background is the produced DSM image from Pix4D, where the interval from lowest to highest pixel value is a rather small range of under 10, making the image difficult to see due to low contrast. Axis is referring to pixel coordinate.

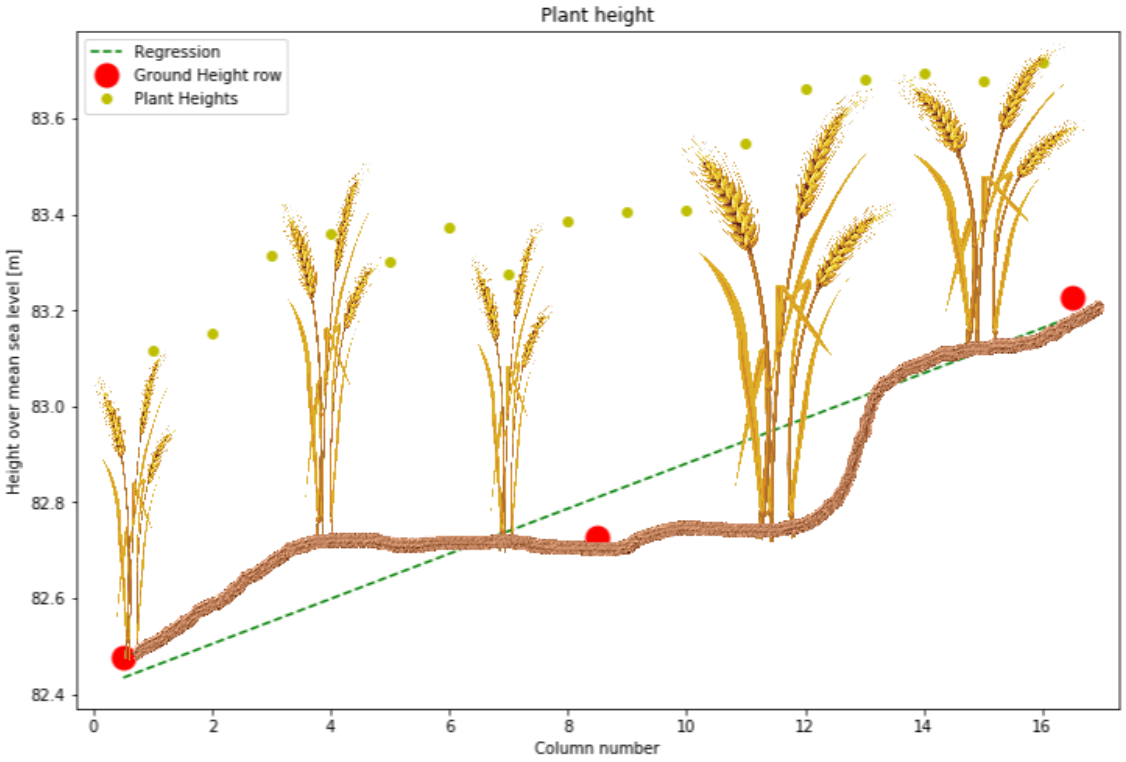

Figure 3.12: A visualization of how ground reference points are measured in the suggested height adjustment regression. The curvature of the ground (brown) is hypothetical, probably exaggerated. Illustration of wheat plants is downloaded from www.pngimg.com.

the height at the ground the plant actually grows. Furthermore when all necessary values are collected, a regression model is fitted by `numpy.polyfit`. The `polyfit` function returns a `numpy.array` whose elements are the polynomial coefficients for the least square polynomial fit (The SciPy community, 2018b). The element named `row_data` is a `pandas.DataFrame` (Pandas, 2018) holding information about ground height measurements for all 27 ground samples in rows and date of the DSM as columns, named `sample`.

Listing 3.2: Regression line from ground height samples.

```
for row_number in range(8):
    ground_measure_columns = np.array([0.5, 8.5, 16.5])
    ground_measure_height = np.array((
        (row_data[sample][row_number+1]+row_data[sample][row_number+2])/2,
        (row_data[sample][row_number+10]+row_data[sample][row_number+11])/2,
        (row_data[sample][row_number+19]+row_data[sample][row_number+20])/2))
    ground_height_regression = np.polyfit(ground_measure_columns,
```

```
                                    ground_measure_height, 1)
```

The height value for the field plots are adjusted accordingly to the regression model by the code listed in Listing 3.2, for each row. A snippet from the code adjusting PH is listed in Listing 3.3. This snippet is placed inside the for loop of Listing 3.2, making the next for loop iterating through the field plots in the specific row. The element named `height_data` is a `pandas.DataFrame` with `'ID'` as the place identifier described in Section 3.1.

The four digit place identifier holds information about row and and column of the field plot, consequently suitable for calculating the adjusted height. The last two digits in the identifier makes up the column number of its field plot. The adjusted data is then calculated by subtracting the value from the rows regression model from the obtained value from the DSM. Note that regression slope, denoted by `ground_height_regression[0]`, is multiplied by the column number plus two. This is to take in to account the two border rows in the test field, both not given identification numbers. Please be advised that the codes listed in listings 3.2 and 3.3 have lines omitted for presenting purpose. Complete code is given in appendix.

Listing 3.3: Adjusting PH values by regression.

```
first_square_in_row = 16*row_number
last_square_in_row = 16 + (16 * row_number)

for k, field_ID in enumerate(
        height_data['ID'][first_square_in_row:last_square_in_row]):
    digitforcol = int(str(field_ID)[2:])
    valuefromdata = height_data[str(sample)][squarenumber+1]
    adjusted_data = valuefromdata - (
        ground_height_regression[0]*(digitforcol+2) +
        ground_height_regression[1])
```

The code for adjusting plant heights was written to be applied on all data obtained from all dates where images was acquired. The code gave reasonable values for PH only for images from August 1st.

3.5.2 Visualization

For simple visual inspection of the computer estimated heights a 3D scatter plot and a 3D bar diagram was used. Python package `matplotlib` provides possibilities for easy plotting in thee dimensions (John Hunter and Darren Dale and Eric Firing and Michael Droettboom and The Matplotlib development team, 2018).

3.6 Statistical Analysis and PCA

As described in Section 3.1 the test site was lied out in an alpha lattice split plot design. This allows the SAS program to perform statistical analysis of variances using the mixed procedure (`PROC MIXED`). The SAS code, which is included in appendix, produces least square means for three groups. Namely the 24 cultivars and one group for the interaction between the cultivars and the fertilizer level for both 8 and 15 kg of nitrogen per daa. The code additionally produced p-values for the null-hypothesis to be true. The null-hypothesis being that there are no difference between the elements within a group. A low p-value can show significance for the findings and thereby rejecting the null-hypothesis. The least square means was calculated for all manually measured heights, including PH, TKW, HLW, DH, DM and GY. Furthermore, least square means for the vegetation indices obtained by the remote sensing apparatus was calculated as well.

Gao et al. (2017) showed that PH is significantly negative correlated to GY and chlorophyll content. Vegetation indices like NDVI and MTCI as means of characteristics for chlorophyll content have shown positive correlation against GY (Zhang and Liu, 2014). Therefor, like Bleken (2017) introduced in his thesis, two parameter which hypothetically correlates with GY was examined. That is dividing cultivars NDVI and MTCI values on their respective value for PH. The parameters where denoted

$$NDVI \times PH^{-1} = \frac{NDVI}{PH} \tag{3.1}$$

where NDVI is the Normalized Differential Vegetation Index, PH is the plant height $[\mathrm{cm}]$ and $\mathrm{NDVI} \times \mathrm{PH}^{-1}$ $[\mathrm{cm}^{-1}]$. Likewise for

$$MTCI \times PH^{-1} = \frac{MTCI}{PH} \tag{3.2}$$

where MTCI is the MERIS Terrestrial Chlorophyll Index, PH is the plant height $[\mathrm{cm}]$ and $\mathrm{NDVI} \times \mathrm{PH}^{-1}$ $[\mathrm{cm}^{-1}]$.

To trace indications of other parameters to correlate either positive or negative, a simple, yet effective, principal component analysis (PCA) tool called `Hoggorm`, visualized by `Hoggormplot`, both developed by Tomic (2018). The PCA used in this thesis follows Oliver Tomic's example on sensory data. For revealing variance in traits of small variations, the data of the traits for this thesis was centered and normalized by subtracting the mean value and dividing by the standard deviation within each trait, before performing PCA.

Chapter 4

Results and Discussion

This chapter will present the findings of the methods used in this thesis. After preparing the material for data extraction, organization of the data found, an interpretation of the findings will follow as an discussion. This thesis, being of an exploratory character, will discuss findings as they are presented.

Due to difficulties in calibrating multispectral images and lack of complete orthomosaic resulted in few dates with valid data for site A. As a result of this, this thesis will focus on data from site B.

4.1 Measurements

4.1.1 NDVI and MTCI

The indices calculated from equations 2.1 and 2.2, for NDVI and MTCI respectively, produced values presented in Figure 4.1 for site B. It shows NDVI values to hold maximum values between day 36 and 54. Comparing with manually measured number of days to heading in range from 47 to 55. This suggest that NDVI values are high in the heading stage, stage 5 in the Zadoks code 2.1, and the flowering stage, which usually occur 10 days after heading stage (Simmons et al., 1995). The data for MTCI values show a clear peak on day 69, (1st of august). This is within the last stages of milk and dough development. As mentioned in section 2.1, high chlorophyll content in these stages is important for final grain yield. MTCI, as an indirect measurement of chlorophyll content, showing

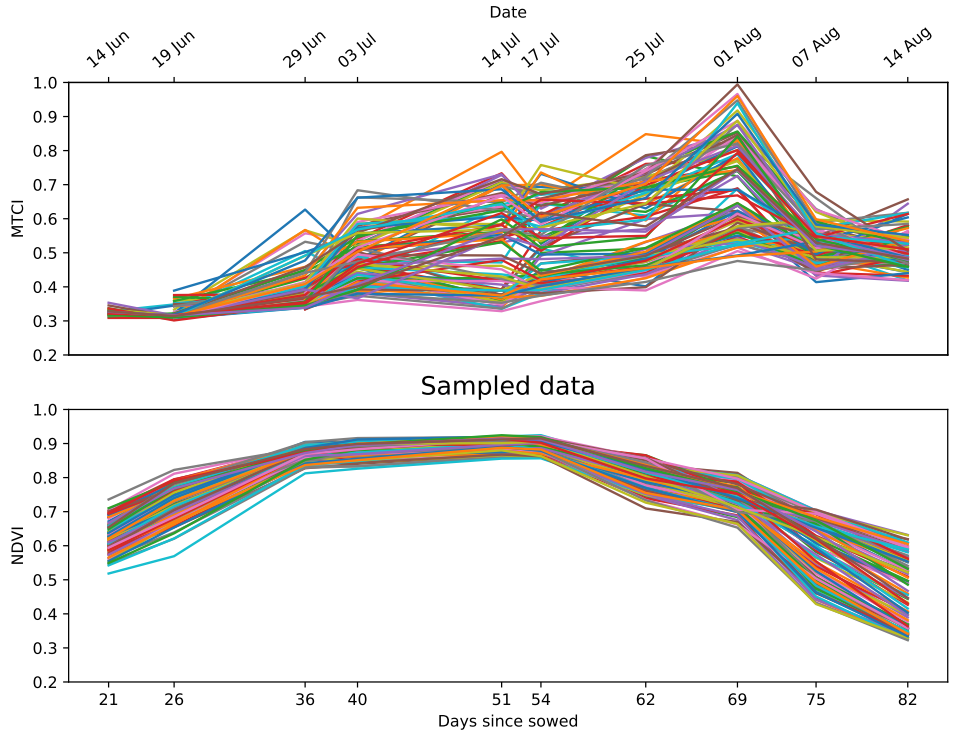

Figure 4.1: Extracted values for MTCI (top) and NDVI (bottom).

high values may predict high grain yield.

The variation in MTCI in Figure 4.1 is more spread out than values for NDVI. Examining Figure 4.2 and Figure 4.3 shows that the different fertilizer levels is an important contributor to this. This speaks for involving REG band in VI calculations to show differences, hence it may better monitor this difference.

Figure 4.3 shows the same data as Figure 4.1, only split into the field plots treated with different level of fertilizer. The differences in values are most clear for MTCI, having far greater values for high level of fertilizer. This is especially clear in the spike seen on day 69 in stage 7 and 8 of the Zadoks code. The differences in NDVI values between the two fertilizer levels is more subtile compared with the differences in MTCI values. Closer studies of the differences for each cultivar, Figure 4.4, show a slightly higher NDVI value for the higher level of fertilizer.

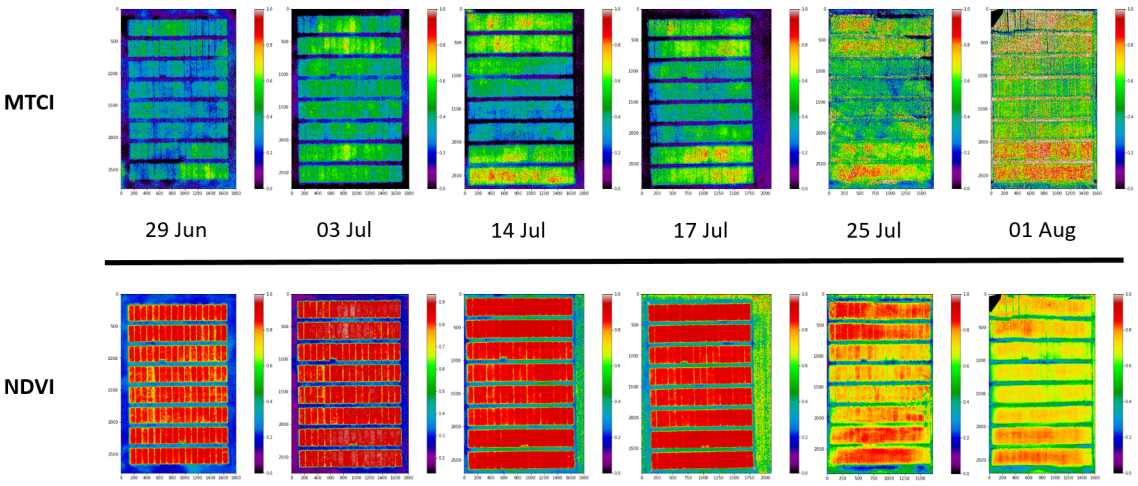

Figure 4.2: Index maps for MTCI (top) and NDVI (bottom) in the period of heading through grain filling.

4.1.2 Estimation of plant height

As described in section 3.5.2, a simple scatter plot in three dimensions, Figure 4.5c, provided an easy way to evaluate data for further analysis. It showed that only DSM from August 1st was a complete data set. It was a serendipity that manual measurements of PH was done on 4th of august. This allowed direct comparison between the computer estimated, Figure 4.5b, and the manual measured PH, Figure 4.5a.

As ripening stage approaches, PH is not changing significantly. The short time between manual measurement and DSM acquirement being nearly optimal for comparison. Observing the Figures 4.5a and 4.5b one can see that the computer estimated PH is about 0.1 to 0.2 meters lower compared to manually measured PH. By subtracting the computer estimated PH value for a field plot from its respective manual measured PH an estimation error plot can be shown (Figure 4.5d). From the error plot, Figure 4.5d, a slight arc across columns can be extracted. This might be a result of the method in which ground height was sampled. Figure 4.6 shows DSM values for PH, in addition to ground sample points and linear regression for the ground in row 18 (furthest north). Note the regression line, which holds the value to subtract from the PH DSM value, lying above the center ground sample point and under both side points, resulting in an higher value to subtract for adjusting PH than the center ground sample would suggest, thus a higher error (Figure 4.5d) at the center of rows.

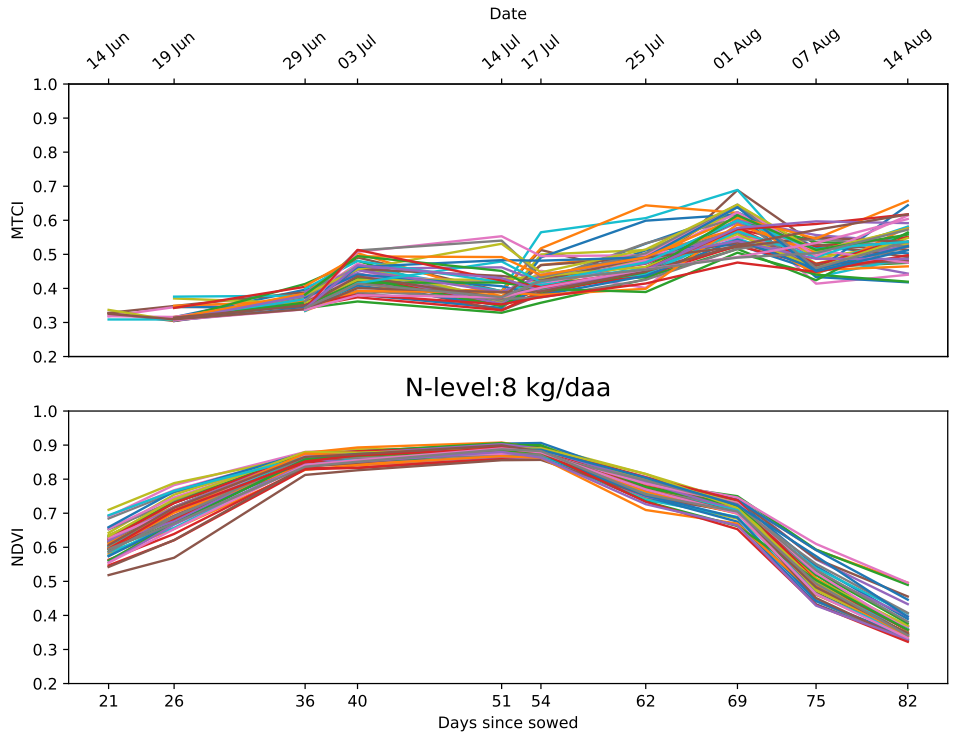

(a) 8 kg/daa

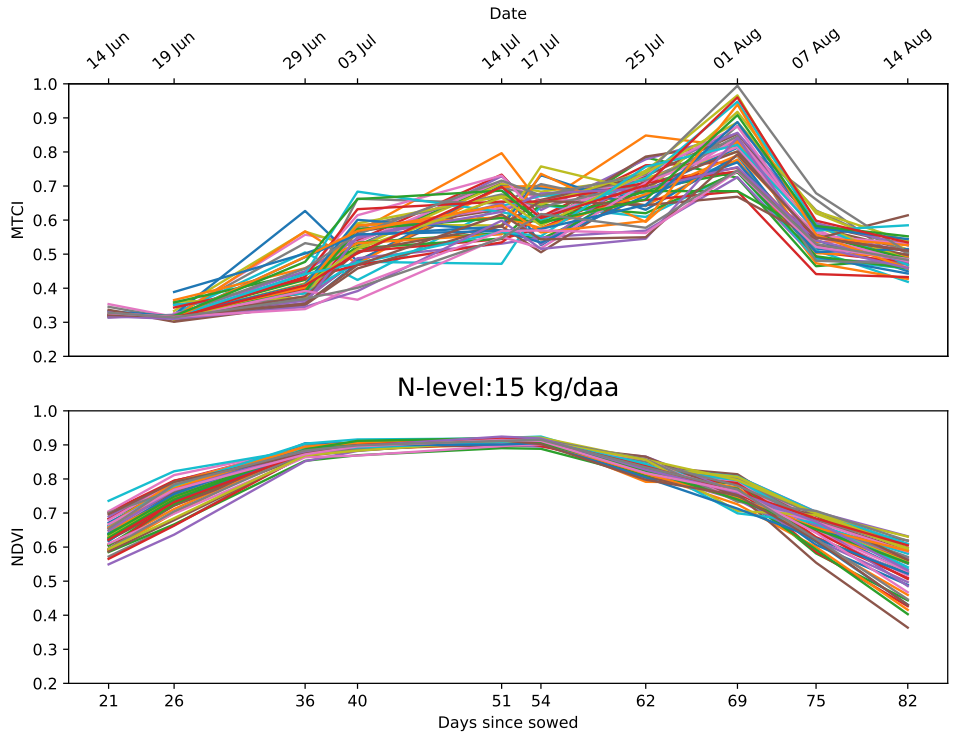

(b) 15 kg/daa

Figure 4.3: Extracted values for MTCI (top) and NDVI (bottom) split into cultivars treated with 8 kg/daa 4.3a and 15 kg/daa 4.3b of Nitrogen

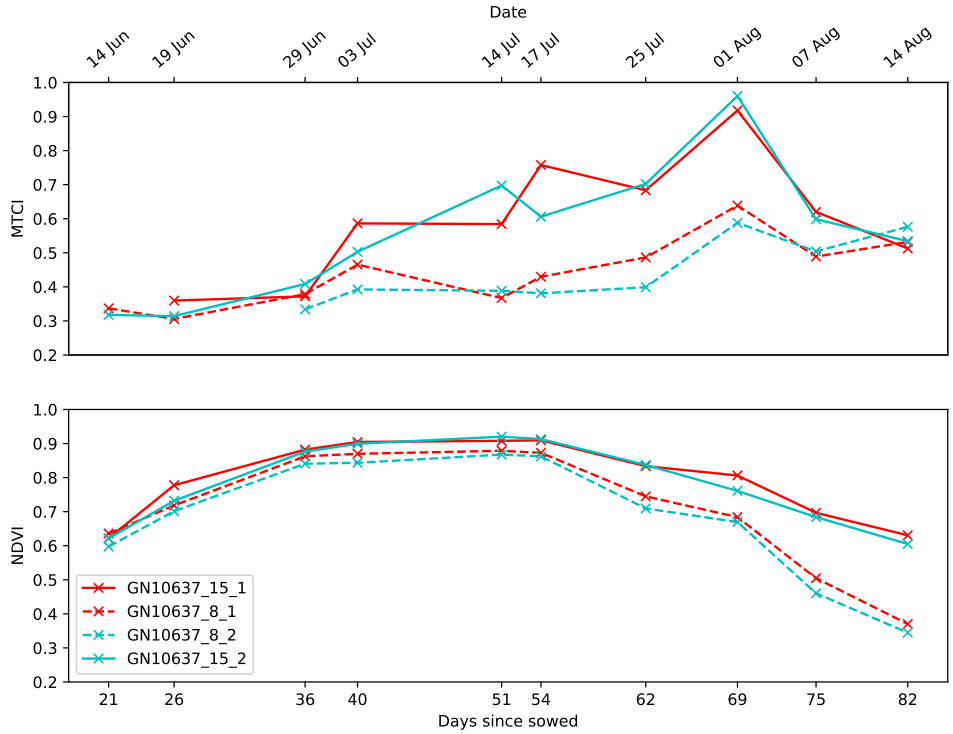

Figure 4.4: Extracted values for MTCI (top) and NDVI (bottom) for cultivar GN10637.

A solution to encountering different errors across columns may be to use a greater number of ground sample points, like Bleken (2017) proposed in his thesis. In fact, when using more points to sample ground height, there will be a possibility to apply a polynomial regression to estimate the ground height where the field plot is planted.

Correlation between the least square means of the manual measured cultivar heights to the computer estimated heights was -0.376. This means that the method for computer estimated height does not reflect the actual height of the cultivars. Bendig et al. (2014) found correlations between manual measured and computer estimated heights as high as 0.92. Such high correlations was obtained by creating a model of the ground height before plant growth.

4.2 Statistical Analysis

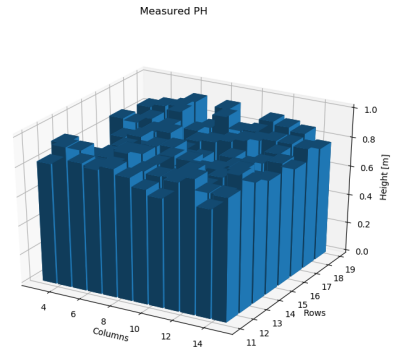

(a) Manually measured

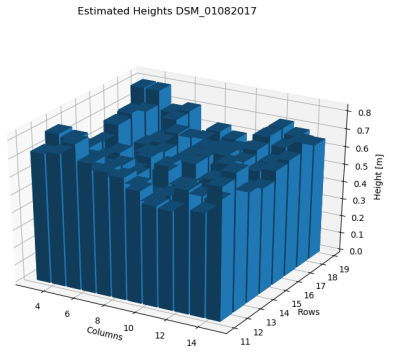

(b) Computer estimated

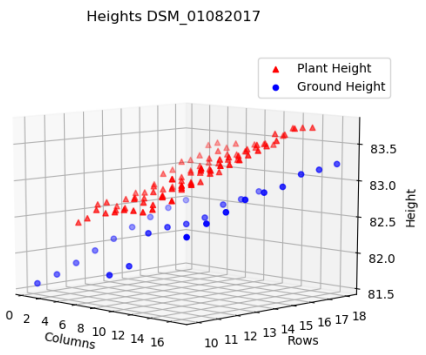

(c) Scatter plot

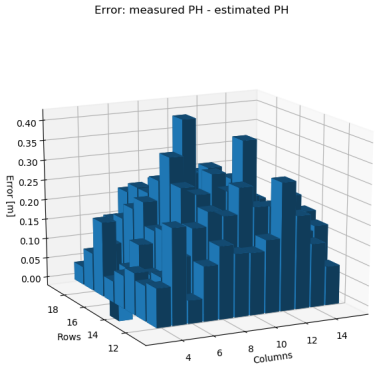

(d) Error

Figure 4.5: Manually measured 4.5a from 4th of august and computer estimated 4.5b heights for 1st of august. The scatter plot 4.5c as described in section 3.5.2. Direct difference between measured and estimated PH in subfigure 4.5d.

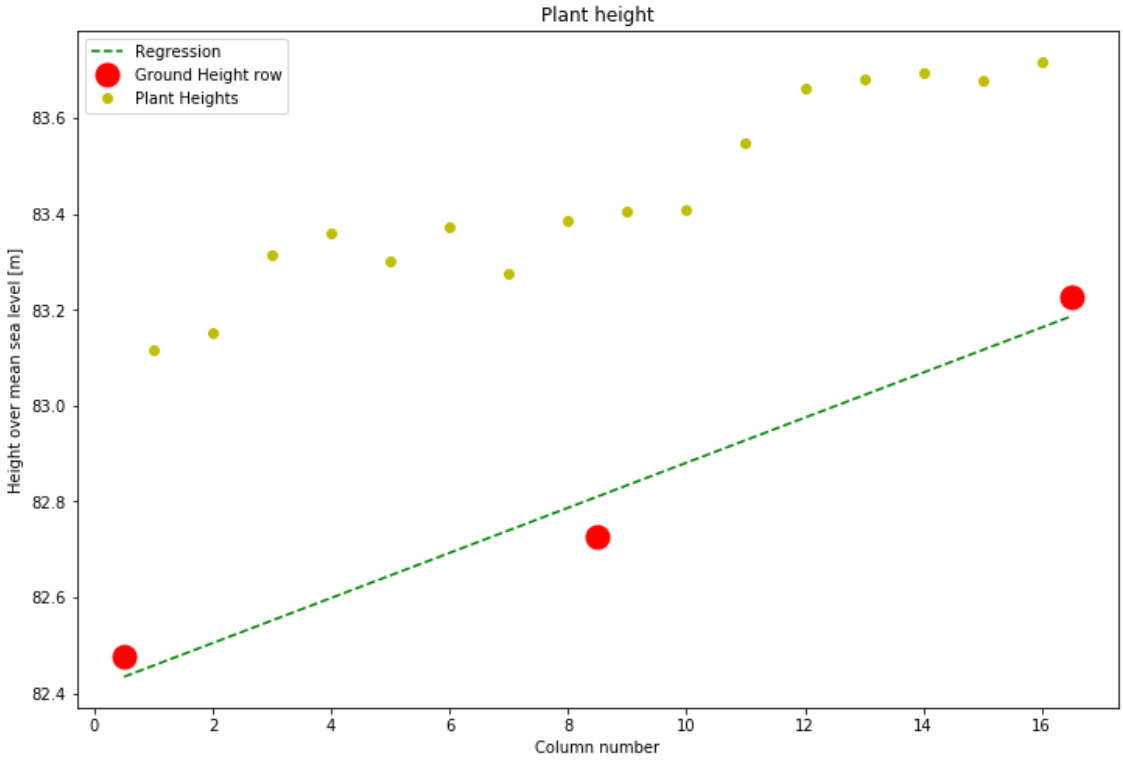

Figure 4.6: Regression line, GRE, made from three ground sample points, red, for each row, together with DSM values of PH obtained 1st of august.

4.2.1 P-values and Least Square Means for Traits

As described in section 3.6, statistical analysis using `PROC MIX` in the SAS software was applied. The output from this method provided p-values. The p-value is the probability finding values that are equally or more extreme than the values observed, given that there is no difference in trait for group sampled. The three groups where cultivars, the level of fertilizer and the interaction between fertilizer level and cultivar. With the model presented in section 2.4 in mind, this reads that the p-value in group *e.g.* $Cultivar \times Nitrogenlevel$ for a trait *e.g.* GY is 0.0002 (from Table 4.1. This means that, since the p-value <0.05, one can say that there is a significant difference in GY for all cultivars given either of the two levels of fertilizer. P-values for the five manually measured traits included in this thesis is presented in Table 4.1. All traits, besides DM, show significance for the cultivar group. For the other two groups, fertilizer level and interaction between cultivar and level of fertilizer, only GY for interaction group shows significance. However GY for fertilizer and TKW for interaction both have p-values right above 0.05 serving as the cut off value.

The SAS-code produced least square means for the three groups. The least square means for the five manually measured traits for site B is presented in Table 5.4 for cultivar group, Table 5.5 for cultivars given 8 kg/daa Nitrogen of fertilizer and Table 5.6 for cultivars given 15 kg/daa Nitrogen of fertilizer.

For site A, there was no different fertilizer level hence only one group of candidates, namely the cultivars. SAS code for site A (given in appendix) estimated the least square means for the two observations of each breed line. For reasons already explained, the dataset for site A was decimated by non-calibrated images and missing image peaces. Although, two dates had both complete and calibrated images. These dates where 1st of June and 14th of July. SAS software-provided p-values for these two is given in Table 4.5. By the Table one can say that dates for NDVI values shows significance to reject the null hypothesis of no difference in between breed lines. MTCI on the other hand does not show sufficient significance to reject the null hypothesis.

Table 4.1: Probabilities for the Null-hypothesis to be true for the groups cultivars, nitrogen levels and cultivars × nitrogen level for the traits, GY, TKW, HLW, DH, DM and manually measured PH at site B.

Group	**GY**	**TKW**	**HLW**	**DH**	**DM**	**PH**
Cultivars	<.0001	<.0001	<.0001	<.0001	0.2642	0.0001
Nitrogen level	0.0531	0.4094	0.5981	0.4183	0.9865	0.1311
Cultivar × Nitrogen level	0.0002	0.0670	0.2227	0.1266	0.5424	0.7299

Table 4.2: p-values fro NDVI and MTCI values observed in site A, 17CMLGI1

	NDVI		MTCI	
date	1. Jun	14. Jul	1. Jun	14. Jul
days since sowed	28	71	28	71
p-value	<.0001	<.0001	0.3082	0.1481

p-values

To show where findings in values for MTCI and NDVI was significant, p-values is plotted, Figure 4.7, for each day measured as the negative logarithmic value to show significant findings. The red line is marking the value for $p = 0.05$, serving as confidence level (CL). Values above the red line indicates significance. Likewise the p-values for the different manual measured traits, the cultivar group is the only group which shows significant findings in almost all observations.

Least Square Means

The estimated values for indices, as least square means, was calculated by the SAS software. Figure 4.8 shows the least square means for the 24 cultivars of NDVI and MTCI. Hence the cultivars being the only group with majority of significant findings, only least square means of cultivar group is presented. One can see the similarities to the raw data, plotted in Figure 4.1, only with an higher MTCI value in June 14th. This might be a result of missing data from some of the values for MTCI, making the value of remaining values to weigh more in the model.

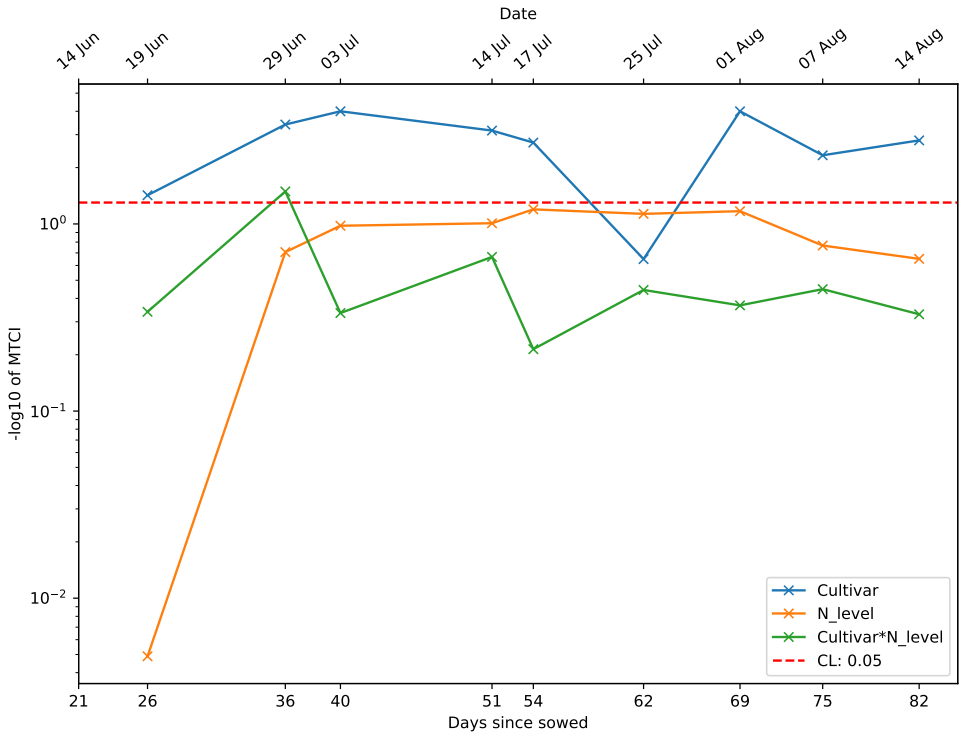

(a) MTCI

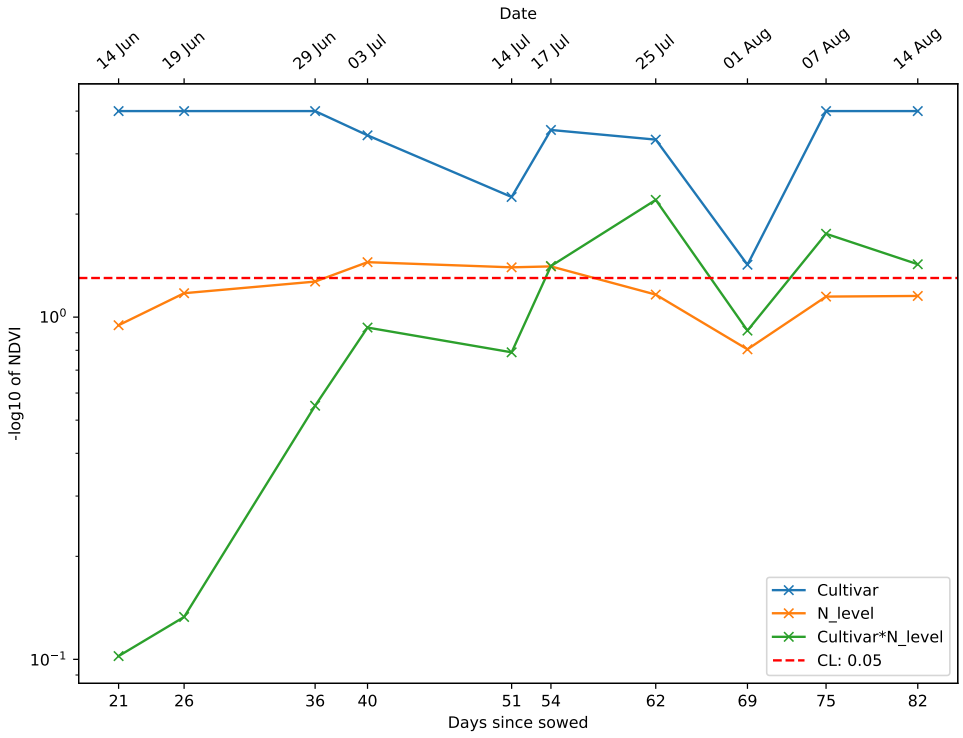

(b) NDVI

Figure 4.7: -log of P-values plotted for the three groups. The red line shows -log og 0.05 to indicate significanc findings

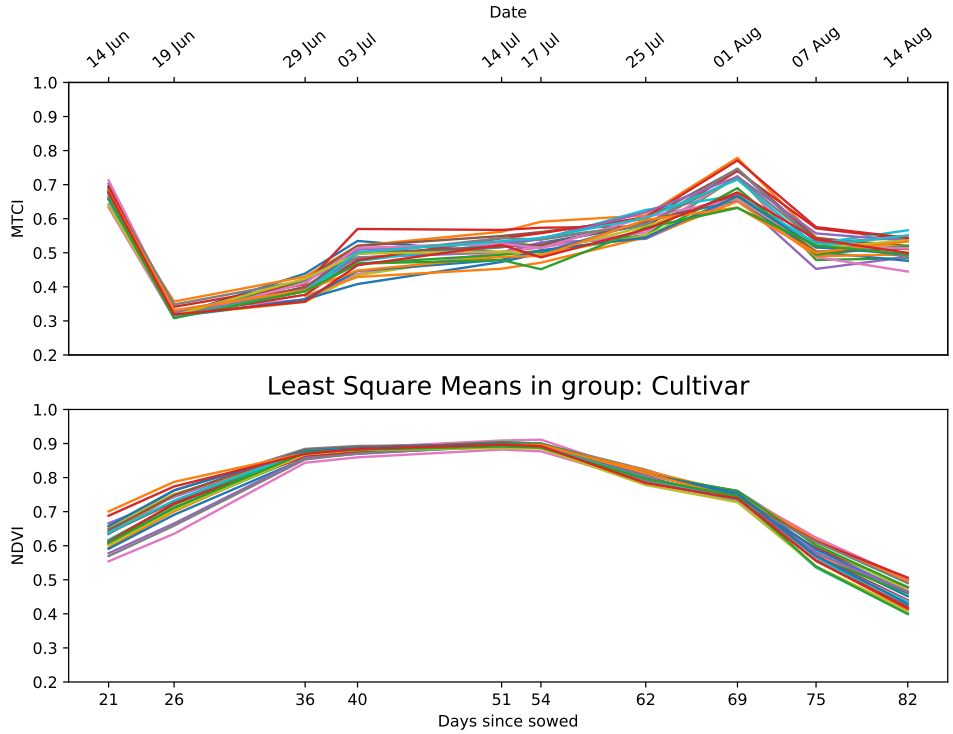

Figure 4.8: Least square means for indices MTCI (top) and NDVI (bottom) for the 24 cultivars.

Correlation

To summarize correlation between the manually measured traits, Pearson correlation coefficients was calculated and are presented in Table 4.4. In Site B there were no strong correlations to GY, >0.5, positive nor negative. Although GY correlate slightly for TKW, DM and PH, 0.337, 0335 and -0,363 respectively. High DM might correspond with a longer milk and dough developing stage, granting longer time for grain weight to grow (Simmons et al., 1995). And negative correlation for GY and PH as lower plants use less energy on transporting nutrients from the soil to the kernel.

NDVI shows to have negative correlation to GY in early season with value -0.417 for the earliest date in the data set. A possible explanation to this is that plants with high values for NDVI in early season mature to early to exploit time for the kernel to develop grain weight. This is specially reflected by the correlation between NDVI in early season and TKW. The time of heading and milk- and dough development shows little to no correlation to GY. This is in the same realm as finding from Gao et al. (2017). MTCI, on the

other hand, shows an opposite pattern in correlation with GY than to that of NDVI, going from slightly positive in early season to slightly negative in late season. The correlations shown by Gao et al. (2017) for MTCI at heading and 10 days after heading was found to be even higher (0.63 and 0.69 respectively) than the findings in this thesis. Zhang and Liu (2014) showed correlations of 0.652 and 0.583 for heading and grain filling respectively. Since MTCI have been shown to indirectly measure content of clorophyll (Zhang and Liu, 2014), and chlorophyll being important for yield production (Simmons et al., 1995), one would expect to see high values for GY for cultivars maintaining high MTCI values through the season, particularly during grain filling period. This is reflected by the data for correlation between MTCI and TKW, where high MTCI in early season may predict high weight for the kernel. However, the earliest measurement for MTCI and TKW correlation contradicts this by having a large negative value, large relative to the other correlations in the matrix. The reason for this may be the missing data for some fields on that date.

For Site A, the significant findings, reportedly by their p-values shown in Table 4.5, shows that only values for MTCI can be said not to be dependent on the cultivar. Looking closer into correlations between the traits, Table 4.6, shows values similar to those seen in Site B. Plants in Site A was planted May 4th and all plants headed in the first week of July, making the measurement of July 14th fall in the period of milk and dough development. This is represented in the high correlation between GY and MTCI of 0.49 for this date. This correlation is considerably larger than that for Site B.

4.2.2 $\mathrm{NDVI} \times \mathrm{PH}^{-1}$ and $\mathrm{MTCII} \times \mathrm{PH}^{-1}$

Recalling new parameters presented in equation 3.1 and 3.2 in Section 3.6, the new parameter $NDVI \times PH^{-1}$ and $MTCI \times PH^{-1}$ was calculated on raw data and SAS software mixed procedure applied for measurements from day 54, July 17th. This date was chosen because of it is situated around heading time, and because of its significant findings for all thee groups in NDVI, however only significant for the cultivar group in MTCI. Due to incomplete sets of data for computer estimated heights manual measurement of PH served as values for this computation in spite of manual measurements was preformed on day 72, 18 days after July 17th. The results of this computation is given in Table 4.3 for group of

Table 4.3: Least square means for indices for cultivars only

	NDVI	MTCI	PH [cm]	NDVI PH $^{-1}$ [cm^{-1}]	MTCI PH $^{-1}$[cm^{-1}]
p-value	0.0003	0.0019	0.0001	0.3284	0.0039
Bjarne	0.900	0.529	72.840	1.12E-02	6.49E-03
Zebra	0.895	0.591	86.820	1.07E-02	7.03E-03
Demonstrant	0.893	0.521	81.077	1.05E-02	6.23E-03
Krabat	0.894	0.574	82.430	1.12E-02	7.05E-03
Mirakel	0.900	0.530	88.393	1.04E-02	6.13E-03
Rabagast	0.891	0.561	74.735	1.19E-02	7.39E-03
Seniorita	0.911	0.515	87.593	1.12E-02	6.33E-03
GN11644	0.899	0.544	77.694	1.12E-02	6.50E-03
GN11542	0.896	0.502	82.578	1.08E-02	5.95E-03
GN13618	0.893	0.539	86.808	1.11E-02	6.70E-03
Arabella	0.891	0.499	82.125	1.02E-02	5.59E-03
GN10521	0.895	0.471	81.456	1.10E-02	5.59E-03
SW01074	0.900	0.506	79.654	1.11E-02	6.09E-03
GN10637	0.889	0.557	77.577	1.13E-02	7.04E-03
SW11230	0.891	0.540	81.862	1.09E-02	6.70E-03
PS-1	0.892	0.523	82.266	1.12E-02	6.68E-03
SW11011	0.877	0.514	84.893	1.03E-02	6.23E-03
SW21074	0.890	0.539	78.757	1.06E-02	6.31E-03
Tjalve	0.885	0.495	77.052	1.10E-02	6.13E-03
Avle	0.893	0.544	81.259	1.02E-02	6.23E-03
Bastian	0.897	0.507	78.854	1.17E-02	6.68E-03
Runar	0.897	0.491	90.441	1.11E-02	6.16E-03
Reno	0.888	0.452	94.063	1.02E-02	5.57E-03
Polkka	0.892	0.486	88.970	1.09E-02	6.07E-03

cultivars only. Pearson correlation matrix for cultivars given 8 kg/daa of nitrogen and for cultivars given 15 kg/daa of nitrogen are given in appendix. The interesting data to look closer on to is the Pearson correlation matrix, Table 4.4

The correlation for the new parameters to GY, presented in Table 4.4, was negative and not noteworthy, <0.15 for the group of cultivars only. Bleken (2017) could report in his thesis positive values of 0.315 using MTCI and 0.221 using NDVI for the same group.

Table 4.4: Pearson correlation matrix for least square means of vegetation indices and manually measured traits in Site B. *p-value for model are <0.05, **p-value for model are <0.01. P-values for correlation models are given in appendix.

	GY	TKW	HLW	DH	DM	PH
TKW	0.337					
HLW	0.066	0.196				
DH	-0.023	-0.211	0.082			
DM	0.335	-0.084	-0.069	0.292		
PH	-0.363*	0.315	0.228	-0.198	-0.386*	
NDVI_14062017	-0.417	-0.511*	0.002	0.115	-0.152	0.195
NDVI_19062017	-0.347	-0.579**	0.038	0.164	-0.109	0.079
NDVI_29062017	-0.202	-0.522*	-0.028	0.144	-0.290	-0.071
NDVI_03072017	-0.113	-0.582**	0.064	0.224	-0.167	-0.071
NDVI_14072017	-0.036	-0.421*	0.090	0.401	0.024	0.010
NDVI_17072017	-0.146	-0.478*	0.105	0.320	0.092	0.040
NDVI_25072017	0.085	-0.207	0.139	-0.206	0.306*	0.029
NDVI_01082017	0.076	-0.244	0.131	0.150	-0.059	0.172
NDVI_07082017	0.188	-0.233	0.104	0.540**	0.568**	-0.176
NDVI_14082017	0.285	-0.081	0.059	0.589**	0.538*	-0.186
MTCI_14062017	0.022	-0.471*	0.164	0.432*	0.304	-0.004
MTCI_29062017	0.215	0.348	-0.061	-0.053	0.003	-0.359*
MTCI_03072017	0.115	0.253	-0.109	0.14	-0.049	-0.293
MTCI_14072017	0.053	0.145	0.158	0.211	-0.002	-0.157
MTCI_17072017	0.127	0.032	0.070	0.232	0.170	-0.356
MTCI_25072017	-0.024	0.304	0.001	-0.336*	0.092	0.046
MTCI_01082017	0.136	-0.126	0.176	0.412	0.298	-0.491**
MTCI_07082017	-0.100	-0.017	-0.021	0.016	0.147	-0.276
MTCI_14082017	-0.133	0.071	-0.108	-0.104	-0.06	-0.158
NDVIxPHˆ(-1)	-0.144	-0.446	0.003	0.255	-0.004	-0.46*
MTCIxPHˆ(-1)	-0.061	-0.067	0.069	0.239	-0.024	-0.374

Table 4.5: p-values fro NDVI and MTCI values observed in site A, 17CMLGI1

Variable	p-value
PlantCover	<.0001
DH	<.0001
DM	<.0001
PH	<.0001
GY	<.0001
NDVI_01062017	<.0001
NDVI_14072017	<.0001
MTCI_01062017	0.3082
MTCI_14072017	0.1481

Table 4.6: Pearson correlation matrix of traits investigated for Site A. *p-value for model are <0.05, **p-value for model are <0.01. P-values for correlation models are given in appendix.

	PlantCover	DH	DM	PH	GY
DH	-0.266**				
DM	-0.403**	0.521**			
PH	0.314**	-0.153**	-0.190**		
GY	0.218**	-0.219**	0.161**	0.072	
NDVI_01062017	0.822**	-0.364**	-0.461**	0.293**	0.320**
NDVI_14072017	0.174**	0.174**	0.136*	0.073	0.335**
MTCI_01062017	0.299**	-0.221**	-0.248**	0.130*	0.124*
MTCI_14072017	0.058	-0.033	0.147*	-0.025	0.490**

4.2.3 PCA

For finding further correlations the simple PCA plotting tool provided a mean of visual evaluation of possible associations. From a PCA's loadings plot, Figure 4.10 and 4.9, one can see traits that supposedly have firm correlation to appear near each other, and traits to have negative correlation appearing diagonally across opposite each other. Due to a relatively small amount of significant findings for groups of fertilizer (N-level) and the interaction between cultivar and level of fertilizer, only loadings for cultivar is presented in loadings plot from site B (4.10). Vegetation indices with low correlations have been held back to improve readability of the loadings plot.

Interpreting Figure 4.10 one can expect to see negative correlations between measurements of NDVI and TKW, as well as for MTCI and PH. In addition to the negative correlation seen in Table 4.4 between GY and PH.

To summarize the differences in correlation between the historical cultivars, Site B, and the younger breed lines, Site A, one can see a clear distinction between vegetation indices before and after heading for the young breed lines. This distinction seem unclear for the historical cultivars.

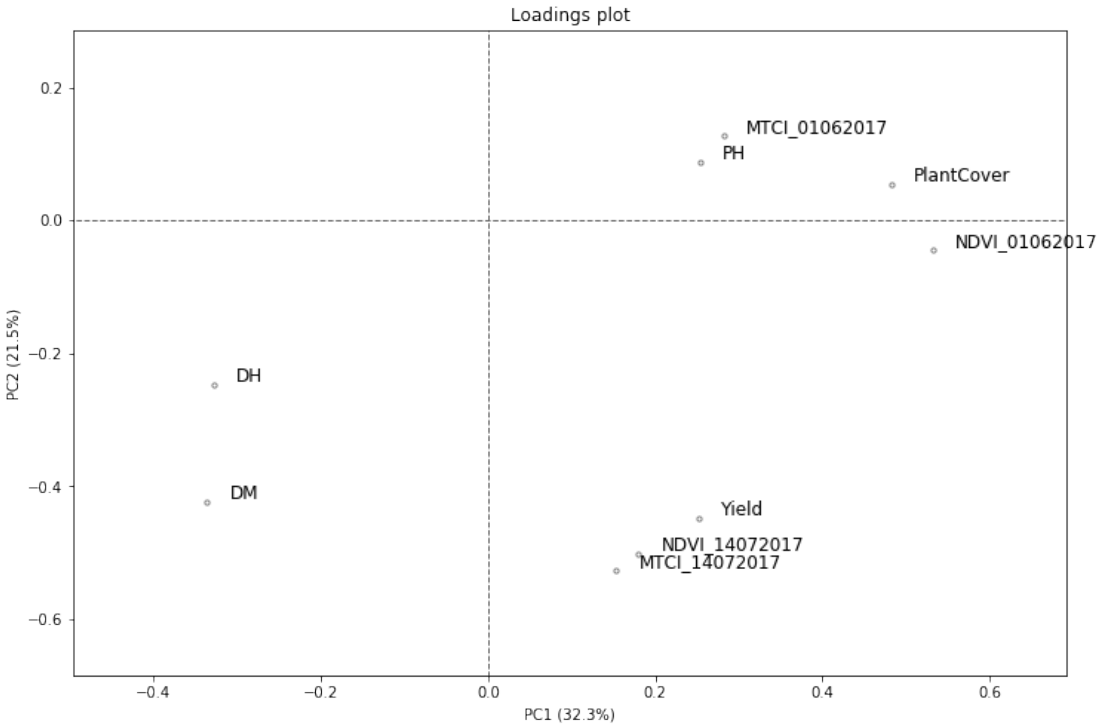

Figure 4.9: Loadings plot prom performed PCA on data from site A with plotting tool by Tomic (2018). Only vegetation indices with the highest correlations to manual measured traits are shown.

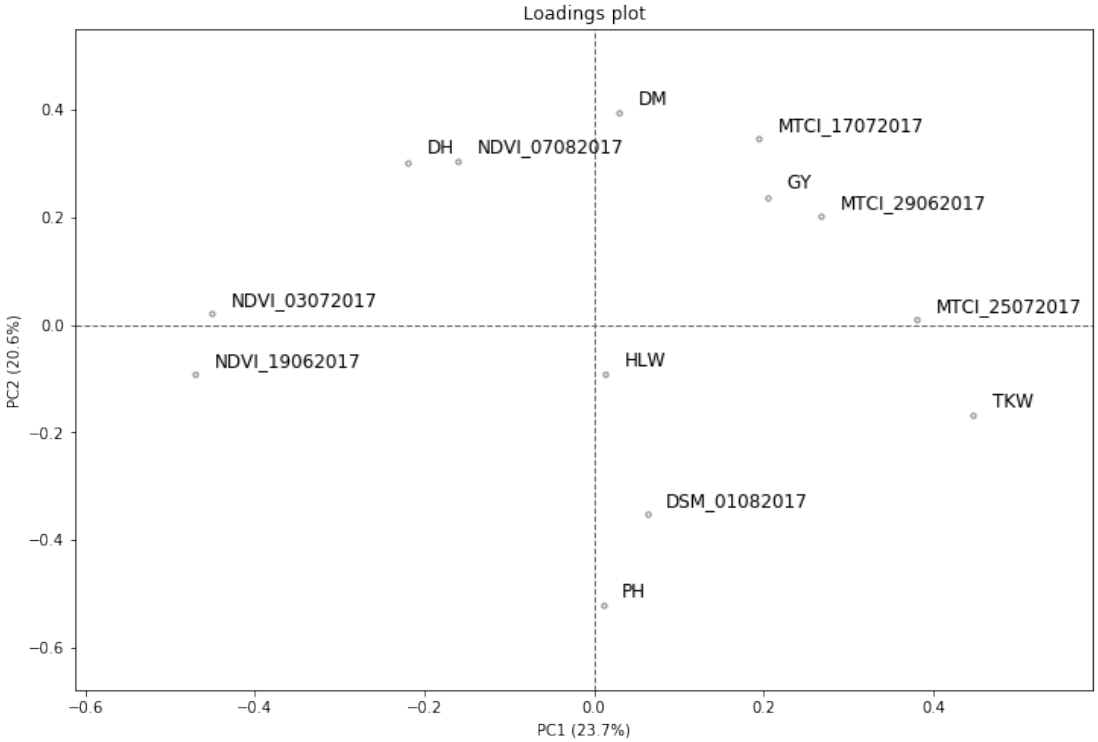

Figure 4.10: Loadings plot prom performed PCA on data from site B with plotting tool by Tomic (2018). Only vegetation indices with the highest correlations to manual measured traits are shown.

4.3 Further Discussion

4.3.1 Calibration

There is one date where Figure 4.1, 4.3 and 4.4 displays a slight increased value, especially for MTCI, namely 1st of August. Values from this date is also standing out in Table 4.4, where they seem to follow the development in values from earlier and later dates. Investigating the quality report from the image processing in Pix4D shows that images for this day where calibrated for the camera only, not taking different illuminations into account. If that where the only circumstance one could expect to see different part of the reflectance images having diverse illuminations as with sparse clouded weather. Inspecting the images from that date, Figure 4.11, yields no clear indications on homogeneous light conditions. However, by inspecting the reflectance image of the RED band, one can see that it is blurred, having the contour lines of soil in between wheat plots smeared out. Soil have a higher value of reflected red light compared to that of vegetation. This blur mixes pixels belonging to vegetation plots with pixels representing soil, producing higher value of RED reflectance for wheat plants for this date. Remembering equation 2.2, where RED reflectance have negative impact on the denominator causing enlargement of the MTCI value.

On the contrary remembering equation 2.1, this hypothesis of an enlarged RED reflectance value would have a negative impact on the value of NDVI, which in Figure 4.1, 4.3, 4.8 and 4.4 is absent.

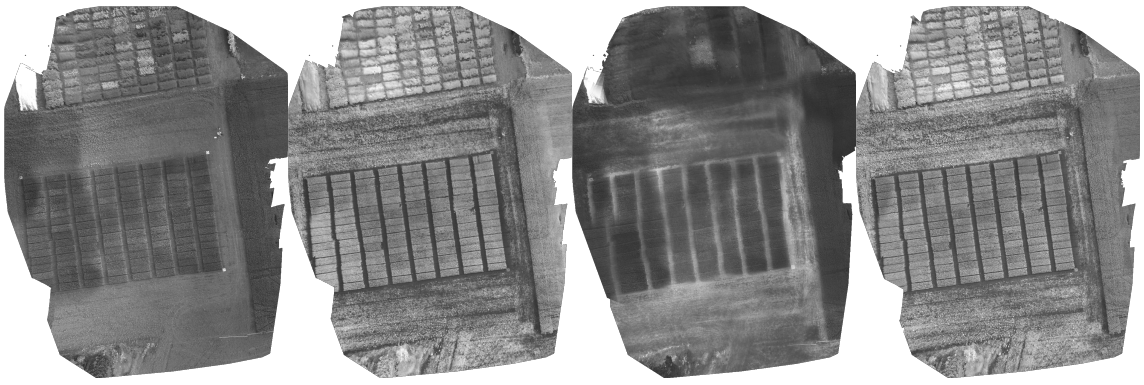

Figure 4.11: Reflectance images for site B 1st of August in four channels from let to right: GRE, NIR, RED and REG. The orientation of these images is rotated 60 degrees counter clocwise.

4.3.2 Data Extraction

Segmentation

In order to make HTP a time saving method for breeders, manually selecting area in the GeoTIFF-image of the field for each field plot is not preferable. Haghighattalab et al. (2016) suggested three methods for obtaining a mask for selecting sought data. First method is a simple grid with cells-length and -width defied by the length and width of the field plots as input. This method obtained reflectance values from the soil in between field plots, in addition to the wanted reflectance values form plant canopy, since the cells was attached to each other. This would lead to similar effects as seen in the RED channel of images from 1st of August (Figure 4.11), where the reflectance value from the canopy have blended with that of the soil. Second method described has a similar approach, besides taking in to consideration the gap between field plots. This method produced separated cells with a defined spacing. Cells was defined to be shorter in length and narrower in width than planted field plots. The third method was based upon the sharp contrast between the reflectance of soil and the reflectance of vegetation in early season, applying the maximum likelihood classifier, also known as the Bayesian classifier, described by the ERDAS Field Guide (ERDAS, Inc, 1999), to classify pixels associated with vegetation as an image mask. Haghighattalab et al. (2016) encountered the same difficulty as in this thesis, that of plants in adjacent field plots identified as one.

A brief effort to make the mask for field plot selections autonomous was done as described in section 3.4.1. The result of this attempt, presented in Figure 4.12, met the same difficulty as Haghighattalab et al. (2016), having multiple field plots merged to one. In Figure 4.12c, NDVI image form July 3rd was used, as it shows the plants mid-growth, having leaf area generally large enough to cover the ground where it was sowed, but not so fully grown to cover gaps in between field plots. One can see plants that have received a higher level of fertilizer, the two rows at the top and the two rows at the bottom in Figure 4.12, being prone to have covered the the gap between field plots. On the other hand, the field plots that received the lower level of fertilizer, the four rows in the middle is prone to not completely cover the ground where it have been planted. In order to obtain values for further statistical analysis, a decision was made to manually define the mask for every

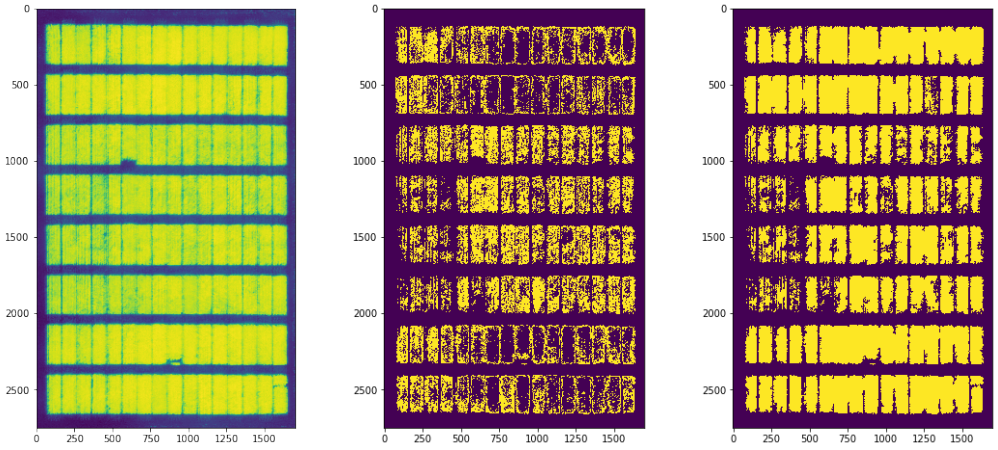

(a) **(b)** **(c)**

Figure 4.12: The process of making a mask to define field plots using NDVI image (4.12a) by applying threshold values (4.12b) decided from inspection of pixel value histogram, to filling holes (4.12c).

field plot.

Chapter 5

Conclusion

In the introduction to this thesis three key questions were stated. After the study of the multispectral signature of spring wheat conducted in the thesis, one can evaluate these key questions.

In this thesis, multispectral images acquired from an UAV was used to generate orthomosaic images of two wheat fields, which in turn were combined to produce the vegetation indices (VIs). The two wheat fields consisted of different cultivars of spring wheat, Site A containing 301 relatively young breed lines, and Site B containing 24 historical cultivars. A considerable amount of time was used to explore alternatives inside the image processing software Pix4D for constructing orthomosaic and DSM images with sufficient quality. The indices for each planted field plot was collected and organized by Python software. The measurements of the two VIs, NDVI and MTCI, were hypothesized to have different correlations to GY trough the season of growth. Differences in correlations were observed in both fields. In addition to the differences in the correlations for VIs and GY within the fields, the two fields exhibited different trends for the correlations to GY.

In Site B, Although the VIs correlations to GY were modest, having absolute value <0.5, a trend could be seen. For NDVI correlations to GY take on negative values in early season, as low as -0.417, and rises trough the season to its peak at 0.285. For MTCIs correlation to GY, one can see an opposite trend to that of NDVI, values are decreasing trough the season of growth. None of the correlations between VIs and GY are shown to

be significant, having the lowest p-value for the intercept at 0.068 for correlation between NDVI at 14th of Jun to GY, which indicates no certain connection.

In Site A, despite having fewer days of observations, clear differences in correlations between VIs and manual measured traits have been shown. For correlation between NDVI and GY takes on similar values, 0.320 and 0.335 successively for the two dates. Both correlations are positive and not changing substantial, in contrast to the change observed in Site B. MTCIs correlations to GY, however, shows an increase in correlation with its highest value of 0.490 for MTCI at 14th of July, about one week after heading occured. All correlations of VIs to GY displays significance, suggesting that there is a connection.

Other correlations between VIs and manual measured traits that are interesting to mention is the correlation between early NDVI measurements and TKW before heading occurs, peaking at -0.582 for measurements from 3rd of July. The slightly negative correlation between early NDVI measurements and DM, speaks for early NDVI to be connected to the extent of the grain filling period. Short grain filling period will result in low average grain weight.

Due to few valid measurements from Site A, there are little data to compare correlations between VIs and GY for historical cultivars and young breed lines. The differences observed shows higher, and significant, for correlations between VIs and GY in Site A, namely the younger breed lines. The correlations found in Site A follows the findings of other studies (Zhang and Liu, 2014; Gao et al., 2017).

The attempt at estimating PH by using DSM with adjusting height by linear regression for ground height did not produce usable results. The correlation between computer estimated PH and manually measured PH was -0.376. In order to improve the computer estimated PH, one could apply more ground measure points and use a polynomial regression to estimate ground height. A solution for estimating more accurate PH may be to calibrate the DSM by GCP with well defined GPS coordinates, particularly for height over MSL. One can benefit from building a calibrated DSM of the site before plants start

to grow. DSM including plants may then be subtracted by the ground DSM direct.

Bibliography

Araus, J. L., Cairns, J. E., 2014. Field high-throughput phenotyping: the new crop breeding frontier. Trends in Plant Science 19 (1), 52 – 61.

Bendig, J., Bolten, A., Bennertz, S., Broscheit, J., Eichfuss, S., Bareth, G., 2014. Estimating biomass of barley using crop surface models (csms) derived from uav-based rgb imaging. Remote Sensing 6 (11), 10395–10412.

Bleken, E. A., 5 2017. A study of different platforms and sensory systems for wheat field trails. Master's thesis, Norwegian University of Life Sciences, Ås, Akershus, Norway.

Burud, I., Lange, G., Lillemo, M., Bleken, E., Grimstad, L., From, P., 07 2017. Exploring robots and uavs as phenotyping tools in plant breeding.

CEMA aisbl - European Agricultural Machinery, 02 2017. Connected agricultural machines in digital farming. Newsletter, Brussels.

Crossa, J., Pérez, P., de los Campos, G., Mahuku, G., Dreisigacker, S., Magorokosho, C., 2011. Genomic selection and prediction in plant breeding. Journal of Crop Improvement 25 (3), 239–261.

Dash, J., Curran, J., Dec 2004. The meris terrestrial chlorophyll index. International Journal of Remote Sensing 25 (23), 5403–5413.

ERDAS, Inc, September 1999. ERDAS Field Guide. ERDAS, Inc., Atlanta, Georgia, fifth edition, revised and expanded Edition.

Esbensen, K. H., Guyot, D., Westad, F., Houmoller, L. P., 2002. Multivariate data analysis: in practice: an introduction to multivariate data analysis and experimental design. Multivariate Data Analysis.

Gamon, J. A., Field, C. B., Goulden, M. L., Griffin, K. L., Hartley, A. E., Joel, G., Peñuelas, J., Valentini, R., 1995. Relationships between ndvi, canopy structure, and photosynthesis in three californian vegetation types. Ecological Applications 5 (1), 28–41.

Gao, F., Ma, D., Yin, G., Rasheed, A., Dong, Y., Xiao, Y., Xia, X., Wu, X., He, Z., 2017. Genetic progress in grain yield and physiological traits in chinese wheat cultivars of southern yellow and huai valley since 1950. Crop Science 57 (2), 760–773.

Hagen, N., Kudenov, M. W., 2013. Review of snapshot spectral imaging technologies. Optical Engineering 52 (9), 090901–090901.

Haghighattalab, A., González Pérez, L., Mondal, S., Singh, D., Schinstock, D., Rutkoski, J., Ortiz-Monasterio, I., Singh, R. P., Goodin, D., Poland, J., Jun 2016. Application of unmanned aerial systems for high throughput phenotyping of large wheat breeding nurseries. Plant Methods 12 (1), 35.

Hykkerud, A., 2017. NDVI EVI eval software. NMBU, Ås, Akershus, 1st Edition.

John Hunter and Darren Dale and Eric Firing and Michael Droettboom and The Matplotlib development team, May 2018. mplot3d api¶. Visited May 13th 2018.
URL `https://matplotlib.org/2.0.2/mpl_toolkits/mplot3d/api.html`

Landbruks- og matdepartementet, 12 2012. St.meld. nr. 9 (2011-2012) - velkommen til bords. Stortingsmelding, Oslo.

LeBoeuf, J., 2000. Practical applications of remote sensing technology—an industry perspective. HortTechnology 10 (3), 475–480.

Mauzerall, D., 1976. Chlorophyll and photosynthesis. Phil. Trans. R. Soc. Lond. B 273 (924), 287–294.

MicaSense, May 2018a. Calibrated reflectance panel. Visited May 13th 2018.
URL https://www.micasense.com/accessories/#!/Calibrated-Reflectance-Panel/p/86371681/category=25401667

MicaSense, May 2018b. Reflectance calibration. Visited May 13th 2018.
URL https://support.micasense.com/hc/en-us/articles/220154947-How-do-calibrated-reflectance-panels-improve-my-data-

Montesinos-López, O. A., Montesinos-López, A., Crossa, J., los Campos, G., Alvarado, G., Suchismita, M., Rutkoski, J., González-Pérez, L., Burgueño, J., 2017. Predicting grain yield using canopy hyperspectral reflectance in wheat breeding data. Plant methods 13 (1), 4.

Pandas, May 2018. Pandas.dataframe. Visited May 13th 2018.
URL https://pandas.pydata.org/pandas-docs/stable/generated/pandas.DataFrame.html

Peñuelas, J., Filella, I., 1998. Visible and near-infrared reflectance techniques for diagnosing plant physiological status. Trends in plant science 3 (4), 151–156.

PEñUELAS, J., FILELLA, I., BIEL, C., SERRANO, L., SAVÉ, R., 1993. The reflectance at the 950 – 970 nm region as an indicator of plant water status. International Journal of Remote Sensing 14 (10), 1887–1905.

Perry Jr, C. R., Lautenschlager, L. F., 1984. Functional equivalence of spectral vegetation indices. Remote sensing of environment 14 (1-3), 169–182.

Peñuelas, J., Pinol, J., Ogaya, R., Filella, I., 1997. Estimation of plant water concentration by the reflectance water index wi (r900/r970). International Journal of Remote Sensing 18 (13), 2869–2875.

Pix4D, May 2018a. Automatic radiometric calibration in pix4d. Visited May 13th 2018.
URL https://support.pix4d.com/hc/en-us/articles/206494883#label2

Pix4D, May 2018b. Image acquisition. Visited May 13th 2018.
URL https://support.pix4d.com/hc/en-us/articles/115002442323-Image-acquisition

Ray, D. K., Ramankutty, N., Mueller, N. D., West, P. C., Foley, J. A., 2012. Recent patterns of crop yield growth and stagnation. Nature Communications 3.

Rouse Jr, J., Haas, R., Schell, J., Deering, D., 1974. Monitoring vegetation systems in the great plains with erts.

Rovira-Más, F., Zhang, Q., Reid, J., Will, J., 2003. Machine vision based automated tractor guidance. International Journal of Smart Engineering System Design 5 (4), 467–480.

Sankaran, S., Khot, L. R., Carter, A. H., 2015a. Field-based crop phenotyping: Multispectral aerial imaging for evaluation of winter wheat emergence and spring stand. Computers and Electronics in Agriculture 118, 372 – 379.

Sankaran, S., Khot, L. R., Espinoza, C. Z., Jarolmasjed, S., Sathuvalli, V. R., Vandemark, G. J., Miklas, P. N., Carter, A. H., Pumphrey, M. O., Knowles, N. R., Pavek, M. J., 2015b. Low-altitude, high-resolution aerial imaging systems for row and field crop phenotyping: A review. European Journal of Agronomy 70, 112 – 123.

Simmons, S., Oelke, E., Anderson, P., 1995. Growth and development guide for spring wheat.

Tattaris, M., Reynolds, M. P., Chapman, S. C., 2016. A direct comparison of remote sensing approaches for high-throughput phenotyping in plant breeding. Frontiers in Plant Science 7, 1131.

The SciPy community, May 2018a. numpy.array. Visited May 13th 2018.
URL https://docs.scipy.org/doc/numpy-1.14.0/reference/generated/numpy.array.html

The SciPy community, May 2018b. numpy.polyfit. Visited May 13th 2018.
URL https://docs.scipy.org/doc/numpy-1.14.0/reference/generated/numpy.polyfit.html

Tomic, O., May 2018. Hoggorm documentation. Visited May 13th 2018.
URL http://hoggorm.readthedocs.io/en/latest/

Tucker, C. J., 1979. Red and photographic infrared linear combinations for monitoring vegetation. Remote sensing of Environment 8 (2), 127–150.

Tudor, May 2018. Ndvi processing. Web article posted October 13, 2017 18:18.
URL https://support.dronesmadeeasy.com/hc/en-us/articles/206003636-NDVI-Processing

Wolfert, S., Ge, L., Verdouw, C., Bogaardt, M.-J., 2017. Big data in smart farming–a review. Agricultural Systems 153, 69–80.

Zadoks, J. C., Chang, T. T., Konzak, C. F., 1974. A decimal code for the growth stages of cereals. Weed research 14 (6), 415–421.

Zhang, S., Liu, L., Aug 2014. The potential of the meris terrestrial chlorophyll index for crop yield prediction. Remote Sensing Letters 5 (8), 733–742.

Appendix

The Appendix consists of NDVI and MTCI plotted for each of the 24 historical cultivars. Further is the 3D visualization of the PH from DSM. Followed by the python source that have been used. Then the collected data for 17BMLROBOT1 is listed. DSM images with psudocolors is then followed by Pearson correlation matrix with respective correlation p-value matrix listed.

5.1 Plotting

5.1.1 NDVI and MTCI for historical cultivars

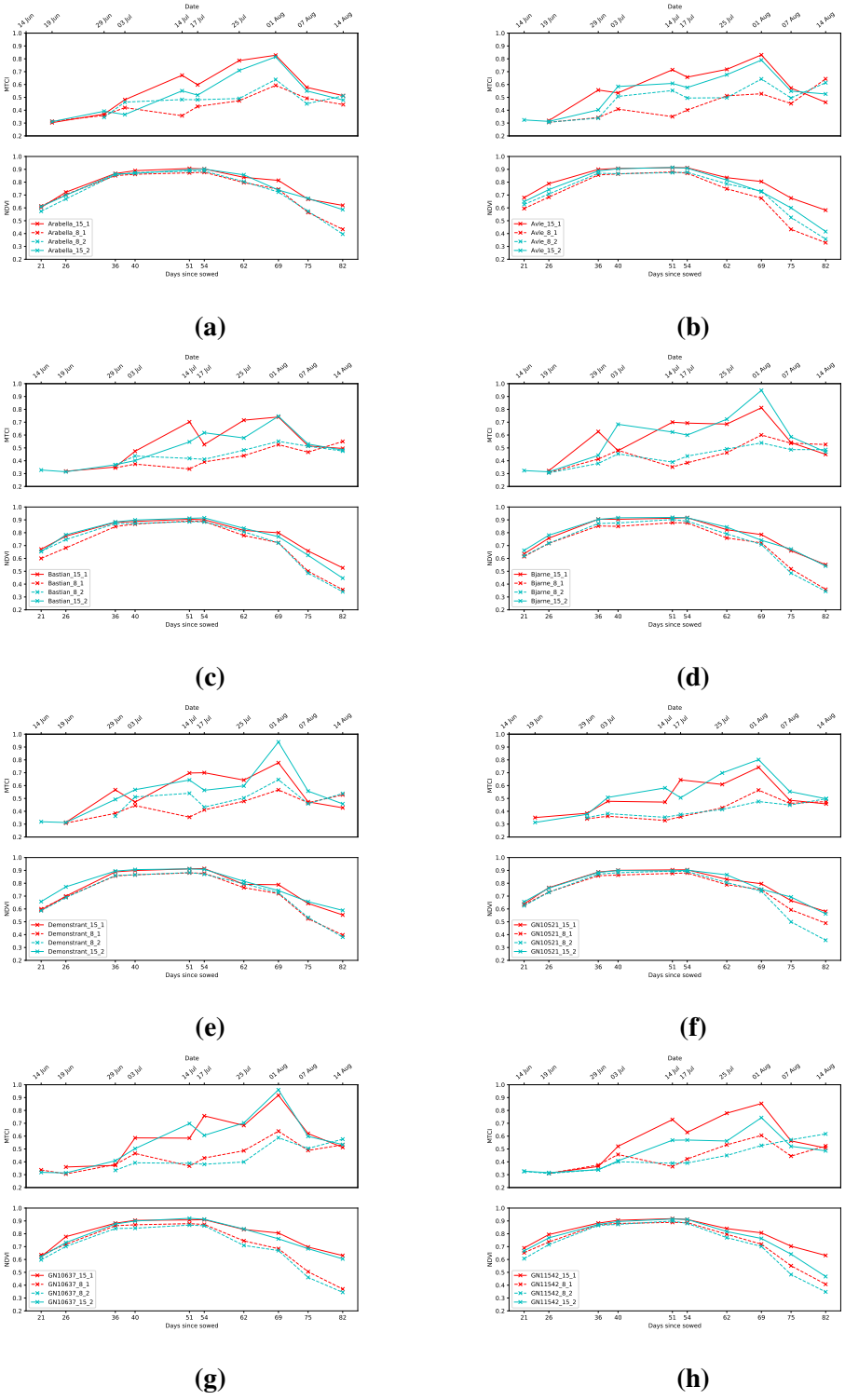

Figure 5.1: Least square means of MTCI and NDVI for all 24 historical cultivars

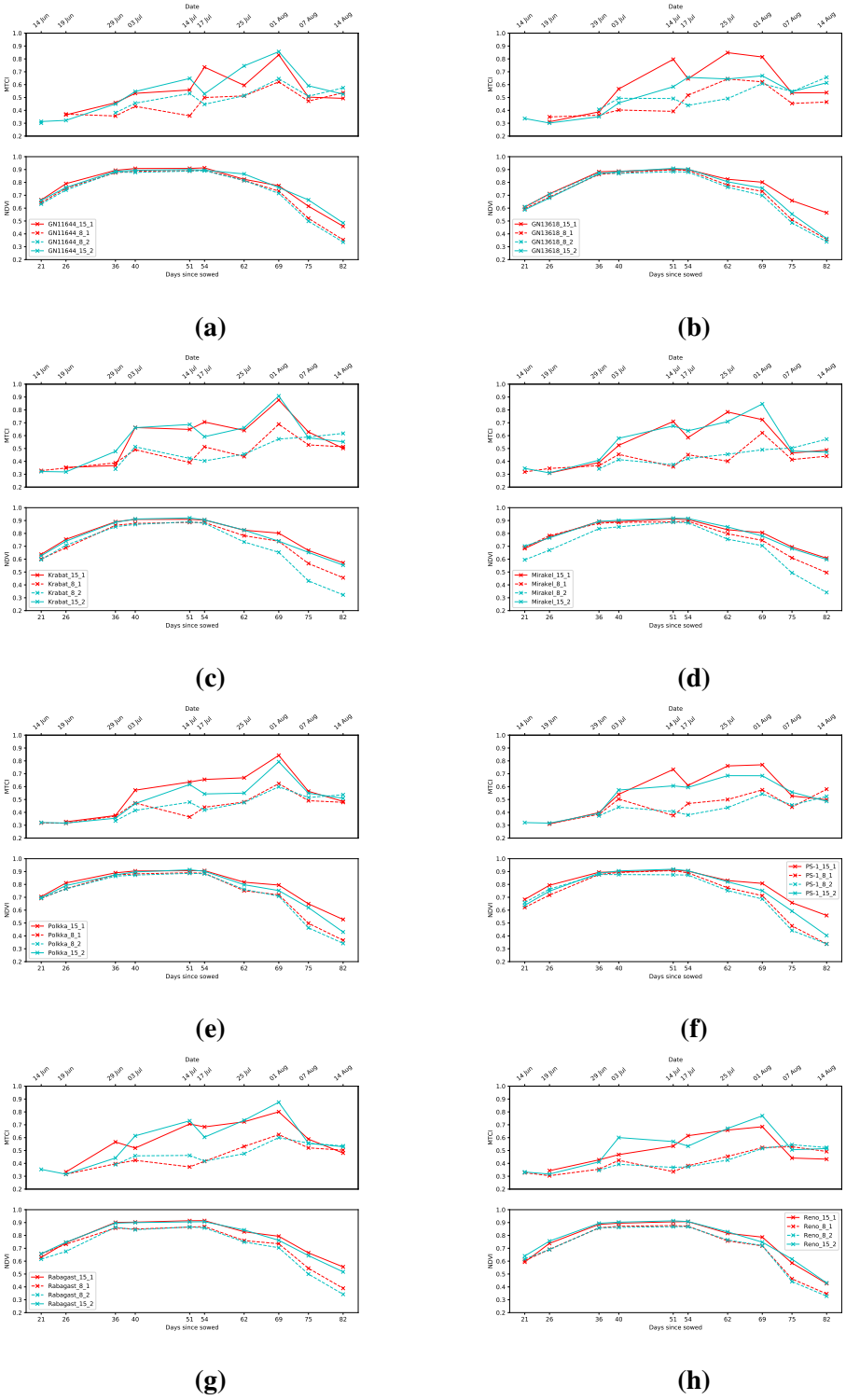

Figure 5.2: Least square means of MTCI and NDVI for all 24 historical cultivars

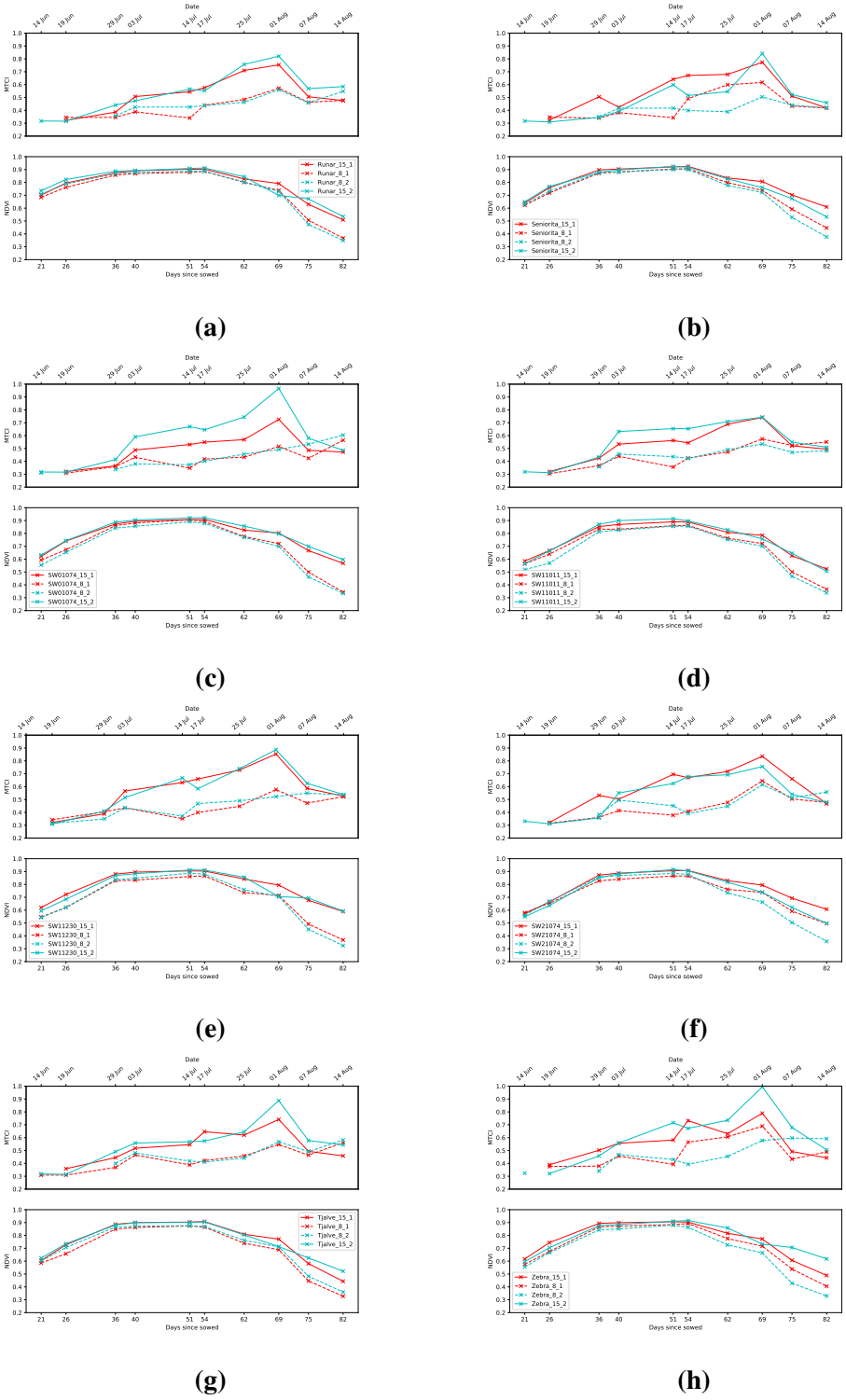

Figure 5.3: Least square means of MTCI and NDVI for all 24 historical cultivars

5.1.2 3D Visualization

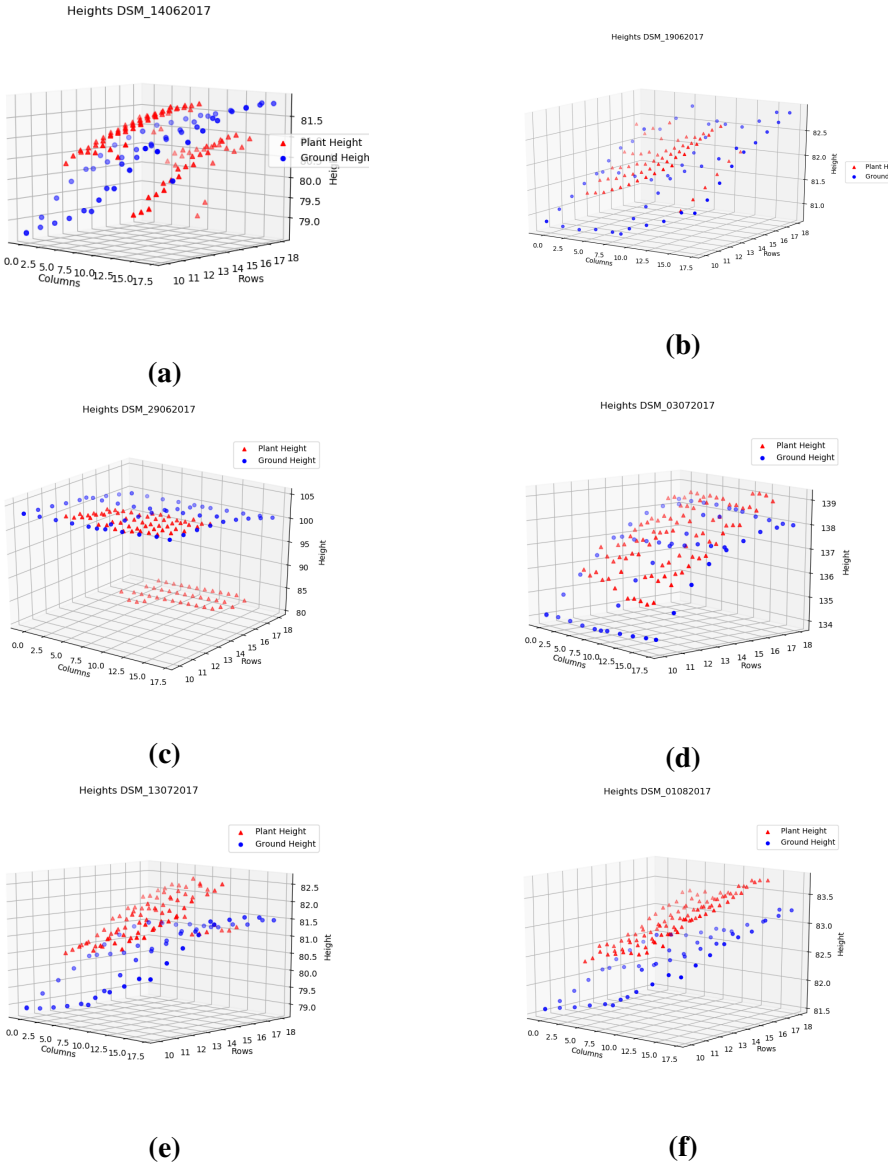

Figure 5.4: 3D visualization of DSM values for PH and ground measure points. Ground points for both rows and columns are shown. This displays the difficulty of handling incomplete DSM data sets.

5.2 Python and SAS code

5.2.1 Value importing and handling

```
"""
The following code is written to handle NDVI and MTCI
form multispectral images of Vollebekk field using python scripts
by Gunnar Lange, Aleksander Hykkerud and Eivind Bleken.


"""

import matplotlib.pyplot as plt
from datetime import datetime
import sys
import os
from os import path
import re
import xlsxwriter
from openpyxl import load_workbook
import numpy as np


fieldname = '0104_Bless/0104_Bless'
NDVI_or_EVI='EVI'
xlsx_or_csv='xlsx'

fields = [n for n in range(128)]

basepath = path.dirname(__file__)
filepath = path.abspath(path.join(basepath, fieldname+'_mean_'+NDVI_or_EVI+
                                  '.txt'))
infile = open(filepath, 'r')
lines = infile.readlines()
infile.close()
working_dir = os.getcwd()

os.chdir("..\..\Vollebekk\Feltkart_Vollebekk_2017" )
wb_names = load_workbook(
    "17BMLROBOT1_-_Avlingsfors k_24_historiske_sorter_Vollebek.xlsx")
fieldbook = wb_names['Feltbok']
os.chdir( working_dir )


# From Eivind Bleken:

NDVI_or_EVI_values = []
```

```
dates = []
squares = []
date_format = '%d-%m-%Y'
for line in lines:
    if line.startswith('Sq.numb:'):
        line = (line.strip()).split(':')
        square = line[1].split()
        squares.append(square[0].strip())
        value = ((line[2].strip()))
        try:
            value = float(value)
            NDVI_or_EVI_values.append(value)
        except ValueError:
            if value == 'EmptySquare':
                NDVI_or_EVI_values.append(np.nan)
            else:
                print('Unknown data encountered')
                print('Unknown data: ' + str(value))
                sys.exit(1)

    elif line.startswith('Image'):
        line = line.split(':')
        line = line[1]
        for s in re.split('[__]', line):
            if s.isdigit():
                line = s[:4]
                dd, mm, YY = line[:2], line[2:4], '2017'
                line = str(dd + '-' + mm + '-' + YY)
                date = datetime.strptime(line, date_format)
                dates.append(date)

    else:
        continue

number_of_squares = int(len(squares) / float(len(dates)))

values = []
for i in range(int(len(NDVI_or_EVI_values)/float(number_of_squares))):
    values.append(NDVI_or_EVI_values[
                  number_of_squares * i : number_of_squares * (i + 1)])

values = [value for (date, value) in sorted(zip(dates, values),
                                            key=lambda pair: pair[0])
          ] #from http://goo.gl/GnBIY
ycoords = []
dates = sorted(dates)
xcoords = [0]
repeated_runs = []
```

```
for j in range(1, len(dates)):
    date_difference = str(dates[j] - dates[0])
    date_difference = date_difference.split()
    if date_difference[0] == '0:00:00':
        repeated_runs.append(j)
    else:
        date_diff = int(date_difference[0])
        if not date_diff in xcoords:
            xcoords.append(date_diff)
        else:
            repeated_runs.append(j)

for k in range(number_of_squares):
    square = []
    for l in range(len(values)):
        if l in repeated_runs:
            continue
        else:
            square.append(values[l][k])
    if square != []:
        ycoords.append(square)

# own produce:

field_rows = 8
field_columns = 16
border_rows = [0, 1, 14, 15]

workbook = xlsxwriter.Workbook(str(fieldname) + '_' + str(NDVI_or_EVI) +
                               '_IDtag_Named.'+ str(xlsx_or_csv))
worksheet = workbook.add_worksheet()
bold = workbook.add_format({'bold': True})

alphabet = 'ABCDEFGHIJKLMNOPQRSTUVWXYZ'

worksheet.write('A1', 'SquareNumber', bold)
worksheet.write('B1', 'ID', bold)
worksheet.write('C1', 'Rep', bold)
worksheet.write('D1', 'N-level', bold)
worksheet.write('E1', 'Name', bold)

for k in range(number_of_squares):
    column = 'A'
    row = k + 2
    worksheet.write(str(column) + str(row), fields[k] + 1)
```

```
field_row_number = 18
field_column_number_start = 1
border_fields = 0
field_column = field_column_number_start

# Cultivar Names as dictionry
cultivar_names = {'Border':'Bastian'}
for l in range(97):
    cultivar_names[str(fieldbook['A' + str(l + 2)].value)] = str(
        fieldbook['I' + str(l + 2)].value)

# Writing ID-tag and Name
for k in range(number_of_squares):
    column = 'B'
    row = k + 2
    column_modulus = k % field_columns
    if column_modulus in border_rows:
        worksheet.write(str(column) + str(row), 'Border')
        worksheet.write('E' + str(row), cultivar_names['Border'])
        border_fields += 1
    else:
        worksheet.write(str(column) + str(row), str(field_row_number) +
                        "{:02}".format(field_column))
        worksheet.write('E' + str(row),
                        cultivar_names[str(field_row_number) +
                                       "{:02}".format(field_column)])
        field_column += 1
    if border_fields % len(border_rows) == 0:
        field_row_number -= 1
        field_column = field_column_number_start

rep_count_start = 5
rep_count = rep_count_start


# Writing repetition count
for k in range(number_of_squares):
    column = 'C'
    row = k + 2
    column_modulus = k % field_columns
    rep_modulus = k % (2 * field_columns)
    if rep_modulus == 0:
        rep_count -= 1
    if not column_modulus in border_rows:
        worksheet.write(str(column) + str(row), str(rep_count))

N_level = 0
rep_count_start = 5
```

```
rep_count = rep_count_start

# Writing Nitrogen level
for k in range(number_of_squares):
    column = 'D'
    row = k + 2
    column_modulus = k % field_columns
    rep_modulus = k % (2 * field_columns)
    if rep_modulus == 0:
        rep_count -= 1
    if rep_count == 4 or rep_count == 1:
        N_level = 15
    elif rep_count == 3 or rep_count == 2:
        N_level = 8
    if not column_modulus in border_rows:
        worksheet.write(str(column) + str(row), str(N_level))

# Writing dates and indices
for number, date in enumerate(dates):
    column = alphabet[number+5]
    row = 1
    worksheet.write(str(column) + str(row),
                    str(NDVI_or_EVI)+'_' + date.strftime('%d') +
                    date.strftime('%m') + date.strftime('%Y'), bold)
    for i, index in enumerate(values[number]):
        row +=1
        worksheet.write(str(column) + str(row), str(index))

# Writing mean values of indices
worksheet.write(str(alphabet[5+len(dates)])+'1', 'Mean_'+str(NDVI_or_EVI), bold)
for square_num, indices in enumerate(ycoords):
    try:
        worksheet.write(str(alphabet[5+len(dates)])+str(square_num+2),
                        str(np.nanmean(indices)))
    except:
        continue


workbook.close()
```

5.2.2 Index Plotting

```
import pandas as pd
import matplotlib.pyplot as plt
import numpy as np
from datetime import date

vi = pd.DataFrame.from_csv(
    'Bless_VI.csv',header=0,sep=';')

sowed = date(2017,5,24)

def day_listmaker(columns, start_date=None):
    if start_date is None:
        start_date = columns[0].split('_')[1]
    dd, mm, YYYY = int(start_date[0:2]), int(start_date[2:4]),
    int(start_date[4:8])
    start_date = date(YYYY,mm,dd)

    days = []

    for d, datestr in enumerate(columns):
        datestr = datestr.split('_')[1]
        dd, mm, YY = int(datestr[:2]), int(datestr[2:4]),
        int(datestr[4:])
        day = date(YY,mm,dd)
        days.append((day-start_date).days)
    return days

def date_listmaker(columns):
    dates = []
    for c, col in enumerate(columns):
        sample_date = col.split('_')[1]
        dd, mm, YYYY = int(sample_date[0:2]), int(sample_date[2:4]),
        int(sample_date[4:8])
        sample_date = date(YYYY,mm,dd)
        dates.append(sample_date.strftime('%d_%b'))
    return dates

NDVI_col = [colname for colname
    in vi.columns if colname.split('_')[0] == 'NDVI']
NDVI_dates = date_listmaker(NDVI_col)
NDVI_days = day_listmaker(NDVI_col, '24052017')

MTCI_col = [colname for colname
    in vi.columns if colname.split('_')[0] == 'MTCI']
MTCI_dates = date_listmaker(MTCI_col)
```

```
MTCI_days = day_listmaker(MTCI_col, '24052017')

index = 'NDVI'

for c, cult in enumerate(cultivars):
    style = {'1':'r','2':'c','15':'-', '8': '--'}
    sub = plt.subplot(111)
    cultivar = vi[vi['Name'] == cultivars[c]]
    n_levels = cultivar['N_level'].tolist()
    reps = cultivar['Rep'].tolist()
    for row in cultivar.iterrows():
        rute, data = row
        n_level = data['N_level']
        rep = data['Rep']
        data = data[eval(index+'_col')].replace('nan', np.nan)
        tag = (cultivars[c] + '_' + str(n_level) + '_' + str(rep))
        sub.plot(eval(index+'_days'),data.tolist(),
        style[str(rep)]+'x'+style[str(n_level)],label=tag)

    sub.set_xticks(eval(index+'_days'))
    sub.set_xticklabels(eval(index+'_dates'), rotation=40)
    sub.set_yticks([0.,0.1,0.2,0.3,0.4,0.5,0.6,0.7,0.8,0.9, 1.])
    sub.set_yticklabels([0.,0.1,0.2,0.3,0.4,0.5,0.6,0.7,0.8,0.9, 1.])
    sub.set_ylabel(index)

    sub.legend()

    plt.show()
```

5.2.3 SAS codes provided by Morten Lillemo

Listing 5.1: SAS code for estimating Least Square Means from 17BMLROBOT1.

```
proc import datafile='c:\sas\2016\16bmlrobotsplit.csv'  out=feltdata replace;
delimiter=';';

proc print;
proc mixed covtest data=feltdata;
class Entry N_level Rep Block Col;
model Avling = entry N_level entry*N_level /outp=resids;
random rep N_level*rep block(N_level*rep) Col /s;
lsmeans  entry N_level entry*N_level ;
ods output LSMeans=lsm;

proc export data=resids outfile='c:\sas\2016\residuals.csv' replace;
delimiter=';';

proc export data=lsm outfile='c:\sas\2016\lsmeans.csv' replace;
delimiter=';';

run;
```

Listing 5.2: SAS code for estimating Least Square Means from 17CMLGI1.

```
proc import datafile='c:\sas\2017\17cmlgi1.csv'  out=dataset replace;
delimiter=',';

proc print;
proc mixed covtest data=dataset;
class Line Rep Block col;
model PlantCover = line /outp=resids;
random rep block(rep) col /s;
lsmeans  line ;
ods output LSMeans=lsm;

proc print data=resids;
var Rute line  rep PlantCover resid;

proc export data=resids outfile='c:\sas\2017\residuals.csv' replace;
delimiter=',';

proc export data=lsm outfile='c:\sas\2017\lsmeans.csv' replace;
delimiter=',';

run;
```

5.2.4 p-values

Listing 5.3: Code for plotting p-values

```
import pandas as pd
import matplotlib.pyplot as plt
import numpy as np
from datetime import date

def day_listmaker... # described

def date_listmaker... # described


NDVI_col = [colname for colname
    in vi.columns if colname.split('_')[0] == 'NDVI']
NDVI_dates = date_listmaker(NDVI_col)
NDVI_days = day_listmaker(NDVI_col, '24052017')

MTCI_col = [colname for colname
    in vi.columns if colname.split('_')[0] == 'MTCI']
MTCI_dates = date_listmaker(MTCI_col)
MTCI_days = day_listmaker(MTCI_col, '24052017')

index = 'NDVI'

pv = pd.DataFrame.from_csv('...\\p_values_MTCI_EVI_NDVI.csv',header=0,sep=';')

sub = plt.subplot(111)

for row in pv.iterrows():

    group, data = row
    data = data[eval(index+'_col')].replace('nan', np.nan)
    tag = (str(group))
    sub.semilogy(sorted(eval(index+'_days')) ,[-np.log10(p) for _, p in sorted(zip(eval(index+'_days'),data
    key=lambda pair: pair[0])],'x-' ,label=tag)

sub.axhline(y=-np.log10(0.05), color='r', linestyle='--', label='CL: 0.05')

scnd = sub.twiny()
scnd.set_xlim(sub.get_xlim())
scnd.set_xticks(eval(index+'_days'))
scnd.set_xticklabels(eval(index+'_dates'), rotation=40)
scnd.set_xlabel('Date')

sub.set_title('p-values for '+index, y=1.16, fontsize=16)
```

```
sub.set_xticks(eval(index+'_days'))
sub.set_xticklabels(eval(index+'_days'))
sub.set_ylabel('-log10 of '+index)
sub.set_xlabel('Days since sowed')

sub.legend()
plt.grid(True, axis='y')

plt.show()
```

Listing 5.4: Code for plotting Least square means and raw data of VIs

```
import pandas as pd
import matplotlib.pyplot as plt
import numpy as np
from datetime import date

raw = pd.DataFrame.from_csv('...Bless_VI.csv',header=0,sep=';')
lsmeans = pd.DataFrame.from_csv('...Vegetation_Indices_lsmeans.csv',header=0,sep=';')

sowed = date(2017,5,24)

def day_listmaker... # described by value handler-code
def date_listmaker... # described by value handler-code

NDVI_col = [colname for colname
    in vi.columns if colname.split('_')[0] == 'NDVI']
NDVI_dates = date_listmaker(NDVI_col)
NDVI_days = day_listmaker(NDVI_col, '24052017')

MTCI_col = [colname for colname
    in vi.columns if colname.split('_')[0] == 'MTCI']
MTCI_dates = date_listmaker(MTCI_col)
MTCI_days = day_listmaker(MTCI_col, '24052017')

index = 'MTCI'

sub = plt.subplot(211)
plottings = data_to_plott
for row in plottings.iterrows():
    rute, data = row
    data = data[eval(index+'_col')].replace('nan', np.nan)
    sub.plot(eval(index+'_days') ,data.tolist())

sub.set_ylim(0.2,1)
sub.set_xticks(eval(index+'_days'))
```

```
sub.set_ylabel(index)

scnd = sub.twiny()
scnd.set_xlim(sub.get_xlim())
scnd.set_xticks(eval(index+'_days'))
scnd.set_xticklabels(eval(index+'_dates'), rotation=40)
scnd.set_xlabel('Date')
sub.tick_params(axis='x',which='both',bottom=False,top=False,labelbottom=False)
sub.set_title('Sampled_data', y=-0.18, fontsize=16)
index = 'NDVI'
sub = plt.subplot(212)
plottings = data_to_plott
for row in plottings.iterrows():
    rute, data = row
    data = data[eval(index+'_col')].replace('nan', np.nan)
    sub.plot(eval(index+'_days') ,data.tolist())

sub.set_ylim(0.2,1)
sub.set_xticks(eval(index+'_days'))
sub.set_xticklabels(eval(index+'_days'))
sub.set_ylabel(index)
sub.set_xlabel('Days_since_sowed')
sub.legend()
plt.show()
```

5.2.5 Correlations

Listing 5.5: Code for calculating Pearson correlations and p-values for the correlations and printing to CSV-files.

```
import pandas as pd
import numpy as np
import codecs
from scipy.stats import pearsonr
import pandas as pd

with codecs.open('17cmlgi1_lsm_VI.csv', "r",encoding='utf-8',
                 errors='ignore') as fdata:
    data = pd.read_csv(fdata, header = 0, sep = ';')

names = set(data['Name'])
data = data.drop(['Line', 'Name'], axis=1)

data.dropna(axis=1, how='any', inplace=True)

NDVI_01062017 = data['NDVI_01062017']
NDVI_14072017 = data['NDVI_14072017']
MTCI_01062017 = data['MTCI_01062017']
MTCI_14072017 = data['MTCI_14072017']

GY = data['GY']
PH = data['PH']
PH = data['PH']
PlantCover = data['PlantCover']

DH = data['DH']
DM = data['DM']

corrmat = np.around(np.corrcoef([PlantCover, DH, DM, PH,GY,
    NDVI_01062017, NDVI_14072017, MTCI_01062017,MTCI_14072017]),decimals=3)[0:,0:5]

C = pd.Index(['PlantCover', 'DH', 'DM', 'PH','GY'],
    name='rows')
I = pd.Index(['PlantCover', 'DH', 'DM', 'PH','GY',
    'NDVI_01062017', 'NDVI_14072017', 'MTCI_01062017',
    'MTCI_14072017'], name='columns')
df = pd.DataFrame(corrmat, index=I, columns=C)
df.to_csv('...\\corrmat.csv',sep=';')

# from https://tinyurl.com/y88nwrkd

def calculate_pvalues(df):
```

```
    df = df.dropna()._get_numeric_data()
    dfcols = pd.DataFrame(columns=df.columns)
    pvalues = dfcols.transpose().join(dfcols, how='outer')
    for r in df.columns:
        for c in df.columns:
            pvalues[r][c] = round(pearsonr(df[r], df[c])[1],5)
    return pvalues

p_value_mat = calculate_pvalues(data[['PlantCover',
    'DH', 'DM', 'PH','GY', 'NDVI_01062017','NDVI_14072017',
    'MTCI_01062017','MTCI_14072017']])[['PlantCover', 'DH',
    'DM', 'PH','GY']]

p_value_mat.to_csv('...\\correlation_p-values_.csv',sep=';')
```

5.2.6 Adjusting DSM

Listing 5.6: Code for adjusting PH from DSM.

```
import xlsxwriter
import numpy as np
import pandas as pd

namebase = '1404_Bless_DSM'
nametale = '_DSM_IDtag_Named'

height_data = pd.DataFrame.from_csv(namebase+'\\'+namebase+nametale+'.csv',
                                    header=0,sep=';')
row_data = pd.DataFrame.from_csv(
    namebase+'/'+namebase+'_Row'+nametale+'.csv',
    header=0,sep=';').dropna(axis=1, how='all')

row_nan = row_data.columns[row_data.isnull().any()].tolist()

height_data.drop(list(set(row_nan)),axis=1)

workbook = xlsxwriter.Workbook(namebase+'/'+namebase+'_adjusted.xlsx')
worksheet = workbook.add_worksheet()
bold = workbook.add_format({'bold': True})

alphabet = 'ABCDEFGHIJKLMNOPQRSTUVWXYZ'

worksheet.write('A1', 'SquareNumber', bold)
worksheet.write('B1', 'ID', bold)
worksheet.write('C1', 'Name', bold)

#Writing Squarenumber, ID and Name
for k, ID in enumerate(height_data['ID']):
    column = 'A'
    row = k + 2
    worksheet.write(str(column) + str(row), str(k))

for k, ID in enumerate(height_data['ID']):
    column = 'B'
    row = k + 2
    worksheet.write(str(column) + str(row), str(ID))

for k, name in enumerate(height_data['Name']):
    column = 'C'
    row = k + 2
    worksheet.write(str(column) + str(row), str(name))

# Adjusting DSM-value
```

```
for t, sample in enumerate([col for col in col_data.columns
                            if col.split('_')[0] == 'DSM']):
    column = alphabet[3 + t]
    worksheet.write(str(column) + str(1), str(sample), bold)
    squarenumber = 0

    for row_number in range(8):
        ground_measure_columns = np.array([0.5, 8.5, 16.5])
        ground_measure_height = np.array((
            (row_data[sample][row_number+1]+row_data[sample][row_number+2])/2,
            (row_data[sample][row_number+10]+row_data[sample][row_number+11])/2,
            (row_data[sample][row_number+19]+row_data[sample][row_number+20])/2)
        ) #mean value of ground sample uver and under wheat field plot
        ground_height_regression = np.polyfit(ground_measure_columns,
                                              ground_measure_height, 1)
        # output is a numpy array where first number is slope number
        # and second is interseption

        first_square_in_row = a = 0+16*row_number
        last_square_in_row = 16 + (16 * row_number)

        for k, field_ID in enumerate(
                height_data['ID'][first_square_in_row:last_square_in_row]):
            row = squarenumber + 2
            if field_ID == 'Border':
                worksheet.write(str(column) + str(row), 'Border')
            else:
                sqnr = field_ID
                digitlist = [int(d) for d in str(sqnr)]
                digitforcol = (digitlist[2] * 10) + digitlist[3]
                if height_data[str(sample)][squarenumber+1] == 'nan':
                    worksheet.write(str(column) + str(row), np.nan)
                elif height_data[str(sample)][squarenumber+1] < (
                        ground_height_regression[0]*(digitforcol+2) +
                        ground_height_regression[1]):
                    worksheet.write(str(column) + str(row), 'Negative')
                else:
                    valuefromdata = height_data[str(sample)][squarenumber+1]
                    adjusted_data = valuefromdata - (
                        ground_height_regression[0]*(digitforcol+2) +
                        ground_height_regression[1])
                    worksheet.write(str(column) + str(row), str(adjusted_data))
            squarenumber += 1
workbook.close()
```

Listing 5.7: Code for producing 3D scatter and bar plot of heights

```
from mpl_toolkits.mplot3d import Axes3D
import numpy as np
import pandas as pd
import matplotlib.pyplot as plt

height_data = pd.DataFrame.from_csv('DSM_DSM_IDtag_Named_raw.csv',header=0,sep=';')
row_data = pd.DataFrame.from_csv('DSM_Row_DSM_IDtag_Named.csv',header=0,sep=';')
estimate_data =  pd.DataFrame.from_csv('DSM_adjusted.csv',header=0,sep=';')

row_data = row_data.dropna(axis=1, how='any')

day = 'DSM_01082017'

fig = plt.figure()
ax = fig.add_subplot(111, projection='3d')

plant_heights = height_data[day]
IDs = height_data['ID']

xs = []
ys = []
zs = []

for ID in height_data['ID']:
    if ID == 'Border':
        continue
    xs.append(int(str(ID)[2:4])+2)
    ys.append(int(str(ID)[0:2]))

for k, height in enumerate(plant_heights):
    if IDs[k+1] == 'Border':
        continue
    if float(height) < 0:
        zs.append(np.nan)
    else:
        zs.append(float(height))

xg = []
yg = []
zg = []

col_set = [0.5, 8.5, 16.5]
f = 1
```

```
for s, col in enumerate(col_set):
    for m in range(9):
        xg.append(col)
        yg.append(9*2-m)
        zg.append(row_data[day][f])
        f += 1

ax.scatter(xs, ys, zs, c='r', marker='^', label='Plant Height')
ax.scatter(xg, yg, zg, c='b', marker='o', label='Ground Height')
ax.set_xlabel('Columns')
ax.set_ylabel('Rows')
ax.set_zlabel('Height')
plt.legend()
fig.suptitle('Heights ' + str(day))
plt.show()

xest = []
yest = []
zest = []

for ID in estimate_data['ID']:
    if ID == 'Border':
        continue
    else:
        xest.append(int(ID[2:4]) + 2)
        yest.append(int(ID[0:2]))

for k, height in enumerate(plant_heights):
    if IDs[k] == 'Border':
        continue
    else:
        zest.append(float(height))

fig = plt.figure()
axm = fig.add_subplot(111, projection='3d')
top = xest + yest
bottom = np.zeros_like(zest)
width = depth = 0.9

axm.bar3d(xest, yest, bottom, width, depth, zest, shade=True)
axm.set_xlabel('Columns')
axm.set_ylabel('Rows')
axm.set_zlabel('Height [m]')
plt.legend()
fig.suptitle('Estimated Heights ' + str(day))
plt.show()
```

5.3 Masking

Listing 5.8: Making a mask for data extraction.

```
import pandas as pd
import matplotlib.pyplot as plt
import scipy
from scipy import ndimage
import cv2
from skimage.morphology import watershed
from skimage.feature import peak_local_max
from matplotlib.image import imread
import sys
import numpy as np
from osgeo import gdal
from PIL import Image

img = gdal.Open('...ndvi.tif')
img = img.ReadAsArray()
img[img<0]=0

def rot_crop_img(image):
    img = scipy.ndimage.rotate(image, -29)
    img = img[2500:5250, 2450:4150]
    return img

ndvi = rot_crop_img(img)
ndvi = ndvi[:,:]
plt.imshow(ndvi)
hist, bin_edges = np.histogram(ndvi, bins=80)
bin_centers = 0.5*(bin_edges[:-1] + bin_edges[1:])
plt.plot(bin_centers,hist)

binary_img_h = ndvi > 0.89
binary_img_l = ndvi < 0.85
binary_img = np.invert(binary_img_h + binary_img_l)
#plt.imshow(binary_img)

fil_img = ndimage.binary_fill_holes(binary_img)

plt.imshow(fil_img)
```

5.4 PCA from Hoggorm-package by Oliver Tomic

Listing 5.9: Code for Producing PCA-loadings plot based on Oliver Tomic' lecture notes for PCA.

```
import pandas as pd
import numpy as np
import hoggorm as hogg
import hoggormplot as hplot
import matplotlib.pyplot as plt
import matplotlib
matplotlib.rcParams['figure.figsize'] = (12, 8)
import codecs

with codecs.open('17cmlgi1_lsm_VI.csv', "r",encoding='utf-8',
                 errors='ignore') as fdata:
    data = pd.read_csv(fdata, header = 0, sep = ';')

names = set(data['Name'])
data = data.drop(['Line', 'Name'], axis=1)

data.dropna(axis=1, how='any', inplace=True)

# from : https://stackoverflow.com/questions/12525722/normalize-data-in-pandas
data_norm = (data-data.mean())/(data.std())

data_array = np.array(data_norm)
DATApca = hogg.nipalsPCA(data_array, 4, cvType = ["loo"])
hplot.loadings(DATApca,comp=[1,2], XvarNames=data.columns.tolist())
```

5.4.1 New Indices Using PH^{-1}

Table 5.1: Least square means for indices gathered July 17th for cultivars given 8 kg/daa Nitrogen.

	NDVI	MTCI	PH [cm]	NDVI PH^{-1} [cm^{-1}]	MTCI PH^{-1}[cm^{-1}]
Bjarne	0.884	0.434	70.444	1.10E-02	5.32E-03
Zebra	0.877	0.473	85.209	1.14E-02	7.67E-03
Demonstrant	0.877	0.434	76.021	1.05E-02	5.58E-03
Krabat	0.883	0.481	83.613	1.10E-02	8.48E-03
Mirakel	0.886	0.420	85.247	1.03E-02	5.08E-03
Rabagast	0.868	0.460	67.658	1.07E-02	7.38E-03
Seniorita	0.903	0.439	83.678	1.12E-02	5.83E-03
GN11644	0.896	0.470	77.213	1.12E-02	8.27E-03
GN11542	0.882	0.405	78.215	1.04E-02	4.88E-03
GN13618	0.884	0.429	82.332	1.05E-02	7.38E-03
Arabella	0.879	0.399	79.853	1.16E-02	5.90E-03
GN10521	0.885	0.370	79.497	1.22E-02	8.87E-03
SW01074	0.885	0.417	79.981	1.16E-02	5.54E-03
GN10637	0.867	0.431	73.677	1.07E-02	7.12E-03
SW11230	0.873	0.436	80.085	1.12E-02	5.69E-03
PS-1	0.877	0.424	80.030	1.12E-02	7.31E-03
SW11011	0.862	0.428	83.310	1.11E-02	5.13E-03
SW21074	0.874	0.426	77.704	1.05E-02	6.77E-03
Tjalve	0.867	0.427	76.313	1.06E-02	4.99E-03
Avle	0.876	0.482	83.041	1.16E-02	8.41E-03
Bastian	0.886	0.405	77.214	9.55E-03	4.16E-03
Runar	0.884	0.401	89.521	1.08E-02	7.03E-03
Reno	0.871	0.373	90.129	1.07E-02	4.32E-03
Polkka	0.884	0.395	86.666	1.13E-02	6.85E-03

Table 5.2: Least square means for indices gathered July 17th for cultivars given 15 kg/daa Nitrogen.

	NDVI	MTCI	PH [cm]	NDVI PH $^{-1}$ [cm^{-1}]	MTCI PH $^{-1}$[cm^{-1}]
Bjarne	0.915	0.625	75.234	1.10E-02	5.01E-03
Zebra	0.913	0.710	88.433	1.12E-02	7.18E-03
Demonstrant	0.909	0.608	86.132	1.10E-02	5.49E-03
Krabat	0.904	0.667	81.251	1.16E-02	8.59E-03
Mirakel	0.914	0.641	91.540	1.15E-02	5.84E-03
Rabagast	0.913	0.662	81.813	1.03E-02	7.57E-03
Seniorita	0.920	0.592	91.509	1.15E-02	5.71E-03
GN11644	0.903	0.618	78.176	1.08E-02	7.66E-03
GN11542	0.910	0.598	86.942	9.16E-03	4.80E-03
GN13618	0.902	0.650	91.285	1.15E-02	7.66E-03
Arabella	0.904	0.599	84.397	1.07E-02	5.08E-03
GN10521	0.906	0.572	83.415	1.05E-02	7.55E-03
SW01074	0.915	0.596	79.327	1.02E-02	5.10E-03
GN10637	0.911	0.684	81.477	1.17E-02	7.16E-03
SW11230	0.909	0.644	83.640	9.88E-03	5.40E-03
PS-1	0.907	0.622	84.502	1.04E-02	7.05E-03
SW11011	0.892	0.600	86.476	1.10E-02	5.19E-03
SW21074	0.906	0.652	79.810	1.25E-02	8.16E-03
Tjalve	0.904	0.563	77.792	1.12E-02	5.05E-03
Avle	0.910	0.605	79.477	1.09E-02	7.27E-03
Bastian	0.909	0.609	80.493	1.00E-02	5.02E-03
Runar	0.909	0.581	91.360	1.03E-02	6.12E-03
Reno	0.906	0.530	97.997	1.14E-02	5.47E-03
Polkka	0.901	0.578	91.273	1.03E-02	6.67E-03

5.5 Collected Data

Table 5.3: Manual collected data, gathered by Bless A. K. Kufoalor, from Site B, 17BMLROBOT1.

Rute	Entry	Name	Plot	N_level [kg/daa]	Rep	Block	PLT	Col	PH [cm]	DH	DM	GY [kg/daa]	TKW [g]	HLW [g]
1101	21	Bastian	1	15	1	1	1	1	82.9	48	104	532.17	33.96	75.5
1102	10	GN13618	2	15	1	1	2	2	98.5	49	104	608.70	38.92	75.5
1103	5	Mirakel	3	15	1	1	3	3	87.6	51	108	570.43	38.87	76.0
1104	16	PS-1	4	15	1	1	4	4	86.6	49	108	690.43	38.79	76.0
1105	9	GN11542	5	15	1	1	5	5	88.1	49	112	657.39	33.43	76.5
1106	11	Arabella	6	15	1	1	6	6	84.5	48	112	756.52	38.88	75.5
1107	20	Avle	7	15	1	2	1	7	78.8	49	110	612.17	32.61	74.5
1108	18	SW21074	8	15	1	2	2	8	75.1	49	110	554.78	34.66	75.5
1109	6	Rabagast	9	15	1	2	3	9	87.8	51	110	582.61	32.04	74.0
1110	7	Seniorita	10	15	1	2	4	10	92.3	53	110	577.39	34.97	77.5
1111	1	Bjarne	11	15	1	2	5	11	74.6	51	110	634.78	35.70	74.0
1112	3	Demonstrant	12	15	1	2	6	12	84.4	51	110	699.13	43.08	79.0
1201	17	SW11011	13	15	1	3	1	1	88.5	48	110	660.87	46.21	76.5
1202	22	Runar	14	15	1	3	2	2	88.6	48	110	610.43	39.64	76.5
1203	13	SW01074	15	15	1	3	3	3	77.4	49	110	662.61	37.10	75.5
1204	15	SW11230	16	15	1	3	4	4	82.4	50	110	678.26	42.56	74.0
1205	24	Polkka	17	15	1	3	5	5	94.1	49	110	606.96	39.44	76.0
1206	4	Krabat	18	15	1	3	6	6	83.1	51	110	673.04	38.89	75.0
1207	14	GN10637	19	15	1	4	1	7	81.8	53	112	697.87	37.05	76.0
1208	12	GN10521	20	15	1	4	2	8	82.6	49	110	617.39	35.68	74.0
1209	2	Zebra	21	15	1	4	3	9	89.1	49	110	565.22	40.94	76.5
1210	8	GN11644	22	15	1	4	4	10	77.4	49	110	591.30	37.98	79.5
1211	19	Tjalve	23	15	1	4	5	11	77.8	51	110	612.17	37.62	73.0
1212	23	Reno	24	15	1	4	6	12	95.9	49	110	570.43	39.54	77.5
1301	6	Rabagast	25	8	2	1	1	1	68.2	49	112	502.61	34.53	75.5
1302	18	SW21074	26	8	2	1	2	2	72.6	49	112	532.17	35.67	77.0

Table 5.3 continued from previous page

Rute	Entry	Name	Plot	N_level [kg/daa]	Rep	Block	PLT	Col	PH [cm]	DH	DM	GY [kg/daa]	TKW [g]	HLW [g]
1303	12	GN10521	27	8	2	1	3	3	80	49	112	499.13	33.73	74.5
1304	17	SW11011	28	8	2	1	4	4	85.1	51	112	490.43	43.87	77.0
1305	11	Arabella	29	8	2	1	5	5	87	48	112	591.30	39.71	76.0
1306	4	Krabat	30	8	2	1	6	6	82	51	112	547.83	36.58	77.0
1307	5	Mirakel	31	8	2	2	1	7	95.4	51	112	532.17	39.56	74.5
1308	22	Runar	32	8	2	2	2	8	88.6	48	112	460.87	38.07	77.0
1309	8	GN11644	33	8	2	2	3	9	73.4	49	112	453.91	37.33	80.0
1310	2	Zebra	34	8	2	2	4	10	81.9	49	112	492.17	38.58	77.0
1311	7	Seniorita	35	8	2	2	5	11	85.5	51	112	467.83	34.31	77.8
1312	10	GN13618	36	8	2	2	6	12	82.9	49	112	521.74	40.24	76.0
1401	1	Bjarne	37	8	2	3	1	1	71.5	51	112	507.83	38.40	74.0
1402	15	SW11230	38	8	2	3	2	2	74.9	49	112	476.52	42.88	75.0
1403	3	Demonstrant	39	8	2	3	3	3	82.2	49	108	561.74	40.99	77.5
1404	23	Reno	40	8	2	3	4	4	91.1	49	108	486.96	36.35	77.5
1405	24	Polkka	41	8	2	3	5	5	86.6	49	108	502.61	36.68	76.0
1406	9	GN11542	42	8	2	3	6	6	81.7	51	112	542.61	36.03	78.0
1407	14	GN10637	43	8	2	4	1	7	76	51	112	492.17	39.26	78.5
1408	19	Tjalve	44	8	2	4	2	8	77	51	112	478.26	38.42	75.5
1409	20	Avle	45	8	2	4	3	9	79.1	51	112	429.57	31.87	73.0
1410	16	PS-1	46	8	2	4	4	10	83.1	51	112	507.83	38.00	77.0
1411	13	SW01074	47	8	2	4	5	11	77.2	51	112	521.74	39.80	77.0
1412	21	Bastian	48	8	2	4	6	12	78.5	51	112	481.74	33.97	76.0
1501	6	Rabagast	49	8	3	1	1	1	67.7	51	112	500.87	34.09	76.0
1502	17	SW11011	50	8	3	1	2	2	81.4	49	112	481.74	46.58	77.0
1503	21	Bastian	51	8	3	1	3	3	75.4	49	112	429.57	34.36	76.0
1504	23	Reno	52	8	3	1	4	4	89.7	49	112	445.22	38.18	77.0
1505	22	Runar	53	8	3	1	5	5	90.5	49	112	474.78	38.60	77.0

Table 5.3 continued from previous page

Rute	Entry	Name	Plot	N_level [kg/daa]	Rep	Block	PLT	Col	PH [cm]	DH	DM	GY [kg/daa]	TKW [g]	HLW [g]
1506	19	Tjalve	54	8	3	1	6	6	75.6	51	112	490.43	37.07	74.0
1507	16	PS-1	55	8	3	2	1	7	77.1	51	112	500.87	38.29	77.0
1508	14	GN10637	56	8	3	2	2	8	71.6	55	112	394.78	37.62	78.5
1509	7	Seniorita	57	8	3	2	3	9	81.9	55	112	405.22	33.28	78.0
1510	12	GN10521	58	8	3	2	4	10	78.7	53	112	471.30	34.86	75.0
1511	1	Bjarne	59	8	3	2	5	11	69.8	51	112	486.96	37.27	73.5
1512	15	SW11230	60	8	3	2	6	12	84.4	51	112	441.74	40.39	75.0
1601	20	Avle	61	8	3	3	1	1	87.2	49	112	476.52	33.69	74.0
1602	3	Demonstrant	62	8	3	3	2	2	69.4	51	112	579.13	39.73	77.0
1603	8	GN11644	63	8	3	3	3	3	80.9	49	112	478.26	38.91	79.8
1604	24	Polkka	64	8	3	3	4	4	87.2	51	112	446.81	34.56	76.0
1605	11	Arabella	65	8	3	3	5	5	73.1	49	112	619.13	40.60	76.5
1606	10	GN13618	66	8	3	3	6	6	81.4	49	112	518.26	38.99	75.5
1607	18	SW21074	67	8	3	4	1	7	82.8	49	112	506.09	37.68	78.0
1608	4	Krabat	68	8	3	4	2	8	85.2	51	112	493.91	37.15	76.5
1609	2	Zebra	69	8	3	4	3	9	88.2	51	112	406.96	39.31	76.0
1610	9	GN11542	70	8	3	4	4	10	74.6	51	112	443.48	32.60	77.0
1611	13	SW01074	71	8	3	4	5	11	83	51	112	480.00	36.71	77.0
1612	5	Mirakel	72	8	3	4	6	12	75	53	112	420.87	37.24	76.5
1701	8	GN11644	73	15	4	1	1	1	79	51	114	622.61	37.78	80.0
1702	12	GN10521	74	15	4	1	2	2	83.7	49	114	676.52	41.13	75.0
1703	6	Rabagast	75	15	4	1	3	3	75.7	51	114	619.13	36.50	77.3
1704	5	Mirakel	76	15	4	1	4	4	95.7	53	114	613.91	43.08	75.8
1705	13	SW01074	77	15	4	1	5	5	81.4	51	114	751.30	39.51	77.5
1706	1	Bjarne	78	15	4	1	6	6	76.1	51	114	671.30	37.84	73.5
1707	23	Reno	79	15	4	2	1	7	100	48	114	596.52	44.10	78.0
1708	20	Avle	80	15	4	2	2	8	80.4	49	114	542.61	36.00	74.0

Table 5.3 continued from previous page

Rute	Entry	Name	Plot	N_level [kg/daa]	Rep	Block	PLT	Col	PH [cm]	DH	DM	GY [kg/daa]	TKW [g]	HLW [g]
1709	16	PS-1	81	15	4	2	3	9	82.6	49	114	606.96	40.08	77.5
1710	17	SW11011	82	15	4	2	4	10	84.5	48	114	631.30	45.32	78.3
1711	18	SW21074	83	15	4	2	5	11	84.5	49	114	612.17	38.24	78.0
1712	10	GN13618	84	15	4	2	6	12	83.2	49	114	575.65	40.16	76.0
1801	11	Arabella	85	15	4	3	1	1	84.7	48	114	700.87	41.46	74.5
1802	2	Zebra	86	15	4	3	2	2	87.3	49	114	612.17	42.57	77.0
1803	15	SW11230	87	15	4	3	3	3	85.1	49	114	603.48	46.31	75.0
1804	22	Runar	88	15	4	3	4	4	94	48	114	560.00	40.56	77.0
1805	19	Tjalve	89	15	4	3	5	5	78.1	51	114	601.74	38.08	73.0
1806	3	Demonstrant	90	15	4	3	6	6	87.5	51	114	720.00	42.06	79.5
1807	4	Krabat	91	15	4	4	1	7	79.9	51	114	674.78	39.87	76.0
1808	14	GN10637	92	15	4	4	2	8	81.4	55	114	622.61	36.87	79.0
1809	7	Seniorita	93	15	4	4	3	9	90.4	53	114	530.43	35.04	78.0
1810	24	Polkka	94	15	4	4	4	10	88.4	53	114	586.09	38.43	76.0
1811	9	GN11542	95	15	4	4	5	11	86.1	51	114	591.30	35.34	75.5
1812	21	Bastian	96	15	4	4	6	12	77.9	48	114	547.83	33.12	75.0

5.5.1 Least Square Means

Site B

Table 5.4: The least square means for traits for all cultivars

Entry	Cultivar	GY [kg/daa]	TKW [g]	HLW [g]	DH	DM	PH [cm]
1	Bjarne	565.260	37.043	73.750	50.599	112.37	72.839
2	Zebra	548.180	40.581	76.625	49.427	111.98	86.821
3	Demonstrant	636.690	41.410	78.250	50.648	111	81.077
4	Krabat	592.690	38.481	76.125	51.121	111.9	82.432
5	Mirakel	526.390	39.630	75.688	52.248	111.55	88.393
6	Rabagast	571.210	34.203	75.688	50.382	112.03	74.735
7	Seniorita	522.480	34.734	77.813	52.453	112.05	87.593
8	GN11644	548.360	37.875	79.813	49.545	111.87	77.694
9	GN11542	548.860	34.503	76.750	50.460	112.99	82.578
10	GN13618	540.790	39.604	75.750	49.068	110.16	86.808
11	Arabella	649.670	40.306	75.625	48.529	112.63	82.125
12	GN10521	575.620	36.389	74.625	49.891	112.03	81.456
13	SW01074	599.280	37.997	76.750	50.861	112.12	79.654
14	GN10637	548.210	37.772	78.000	53.439	112.46	77.577
15	SW11230	551.130	42.939	74.750	49.663	112.2	81.862
16	PS-1	579.310	38.794	76.875	49.587	111.57	82.266
17	SW11011	566.260	45.440	77.188	48.960	111.81	84.893
18	SW21074	553.820	36.654	77.125	49.286	111.87	78.757
19	Tjalve	542.880	37.730	73.875	51.191	111.94	77.052
20	Avle	524.380	33.429	73.875	49.416	111.73	81.259
21	Bastian	502.220	33.909	75.625	48.849	110.54	78.854
22	Runar	522.170	39.132	76.875	48.563	111.89	90.441
23	Reno	510.840	39.340	77.500	48.754	110.76	94.063
24	Polkka	515.570	37.264	76.000	50.562	111.04	88.970

Table 5.5: The least square means for traits for all cultivars given 8 kg/ha of Nitrogen

Entry	Cultivar	GY [kg/daa]	TKW [g]	HLW [g]	DH	DM	PH [cm]
1	Bjarne	493.770	37.519	73.750	50.447	112.8	70.444
2	Zebra	484.790	39.286	76.500	49.894	111.99	85.209
3	Demonstrant	561.790	39.955	77.250	50.499	110.22	76.021
4	Krabat	538.440	37.435	76.750	51.011	111.95	83.613
5	Mirakel	465.400	38.517	75.500	52.535	111.71	85.247
6	Rabagast	510.750	34.288	75.750	49.873	112.1	67.658
7	Seniorita	457.490	33.916	77.875	52.637	112.13	83.678
8	GN11644	492.220	38.152	79.875	49.493	111.69	77.213
9	GN11542	492.720	34.380	77.500	50.801	112.45	78.215
10	GN13618	500.550	39.742	75.750	49.138	111.37	82.332
11	Arabella	574.400	40.330	76.250	49.211	111.67	79.853
12	GN10521	508.810	34.661	74.750	50.881	112.18	79.497
13	SW01074	504.100	38.170	77.000	51.047	112.23	79.981
14	GN10637	439.500	38.338	78.500	52.700	112.06	73.677
15	SW11230	446.830	41.468	75.000	49.428	112.35	80.085
16	PS-1	492.260	38.051	77.000	50.591	112.09	80.030
17	SW11011	479.310	45.350	77.000	49.969	111.74	83.310
18	SW21074	507.230	36.912	77.500	49.521	111.95	77.704
19	Tjalve	487.360	37.631	74.750	50.842	111.78	76.313
20	Avle	469.530	32.668	73.500	49.499	111.82	83.041
21	Bastian	466.410	33.942	76.000	50.234	111.7	77.214
22	Runar	465.160	38.215	77.000	49.106	111.79	89.521
23	Reno	454.120	37.012	77.250	48.574	110.14	90.129
24	Polkka	444.380	35.371	76.000	50.071	110.08	86.666

Table 5.6: The least square means for traits for all cultivars given 15 kg/ha of Nitrogen

Entry	Cultivar	GY [kg/daa]	TKW [g]	HLW [g]	DH	DM	PH [cm]
1	Bjarne	636.750	36.568	73.750	50.750	111.95	75.234
2	Zebra	611.560	41.875	76.750	48.960	111.97	88.433
3	Demonstrant	711.590	42.864	79.250	50.798	111.77	86.132
4	Krabat	646.930	39.526	75.500	51.231	111.85	81.251
5	Mirakel	587.380	40.744	75.875	51.960	111.38	91.540
6	Rabagast	631.680	34.119	75.625	50.891	111.96	81.813
7	Seniorita	587.460	35.552	77.750	52.270	111.97	91.509
8	GN11644	604.510	37.598	79.750	49.597	112.05	78.176
9	GN11542	605.000	34.626	76.000	50.118	113.53	86.942
10	GN13618	581.030	39.466	75.750	48.998	108.95	91.285
11	Arabella	724.930	40.281	75.000	47.846	113.59	84.397
12	GN10521	642.420	38.117	74.500	48.902	111.88	83.415
13	SW01074	694.450	37.824	76.500	50.674	112	79.327
14	GN10637	656.910	37.206	77.500	54.179	112.87	81.477
15	SW11230	655.430	44.411	74.500	49.897	112.06	83.640
16	PS-1	666.370	39.537	76.750	48.583	111.06	84.502
17	SW11011	653.210	45.530	77.375	47.952	111.88	86.476
18	SW21074	600.410	36.396	76.750	49.051	111.8	79.810
19	Tjalve	598.410	37.829	73.000	51.539	112.09	77.792
20	Avle	579.220	34.191	74.250	49.333	111.64	79.477
21	Bastian	538.040	33.876	75.250	47.464	109.37	80.493
22	Runar	579.180	40.048	76.750	48.020	111.99	91.360
23	Reno	567.550	41.667	77.750	48.934	111.37	97.997
24	Polkka	586.760	39.158	76.000	51.053	112.01	91.273

5.6 DSM Images

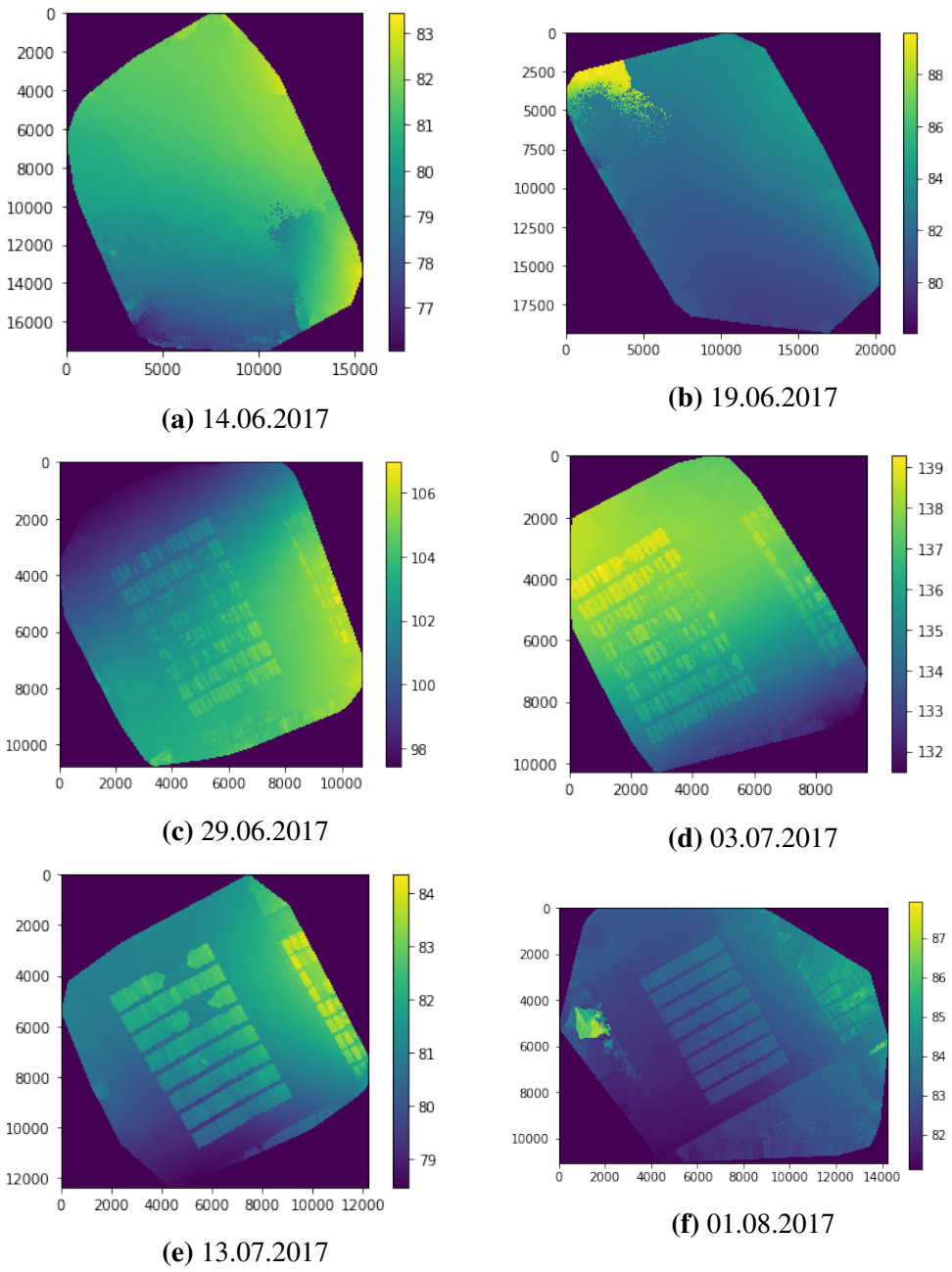

(a) 14.06.2017

(b) 19.06.2017

(c) 29.06.2017

(d) 03.07.2017

(e) 13.07.2017

(f) 01.08.2017

Figure 5.5: DSM images: One can see anomalies from shear in the rayCloud in Pix4D in images from June 14th and 19th.

5.6.1 Collected

Parson correlation Matrix

Table 5.7: P-values for the Pearson correlation matrix of traits investigated for Site A.

	PlantCover	DH	DM	PH	GY
DH	<0.001				
DM	<0.001	<0.001			
PH	<0.001	0.008	0.001		
GY	<0.001	<0.001	0.005	0.214	
NDVI_01062017	<0.001	<0.001	<0.001	<0.001	<0.001
NDVI_14072017	0.002	0.002	0.018	0.206	<0.001
MTCI_01062017	<0.001	<0.001	<0.001	0.024	0.032
MTCI_14072017	0.313	0.563	0.011	0.672	<0.001

Table 5.8: Pearson correlation matrix for least square means of vegetation indices and manually measured traits. Computed for cultivars given 8 kg/daa Nitrogen fertilizer.

	GY	TKW	HLW	DH	DM	PH
TKW	0.337					
HLW	0.066	0.196				
DH	-0.023	-0.211	0.082			
DM	0.335	-0.084	-0.069	0.292		
PH	-0.363	0.315	0.228	-0.198	-0.386	
NDVI_14062017	0.009	0.065	-0.043	-0.153	0.116	-0.003
NDVI_19062017	-0.042	0.058	0.034	-0.057	0.111	-0.016
NDVI_29062017	0.054	-0.004	-0.138	0.021	0.047	-0.056
NDVI_03072017	-0.173	-0.124	0.096	0.018	-0.056	-0.007
NDVI_14072017	-0.169	-0.159	0.119	0.093	0.021	-0.109
NDVI_17072017	-0.134	-0.155	0.09	0.07	-0.003	-0.072
NDVI_25072017	-0.331	-0.038	0.142	-0.165	-0.191	0.168
NDVI_01082017	-0.25	-0.233	0.065	-0.156	-0.134	0.055
NDVI_07082017	-0.16	-0.207	0.307	-0.07	-0.116	0.058
NDVI_14082017	-0.146	-0.168	0.324	-0.017	-0.122	0.087
MTCI_14062017	-0.224	-0.151	0.229	-0.085	-0.154	0.095
MTCI_19062017	0.352	0.142	0.229	0.234	0.161	-0.178
MTCI_29062017	0.234	-0.076	-0.073	-0.063	0.096	-0.132
MTCI_03072017	0.184	-0.169	0.075	0.052	0.086	-0.246
MTCI_14072017	0.023	-0.226	0.125	-0.045	-0.022	-0.137
MTCI_17072017	0.049	-0.187	0.083	-0.033	-0.013	-0.084
MTCI_25072017	-0.035	-0.092	0.01	-0.149	-0.125	-0.044
MTCI_01082017	0.121	-0.082	0.166	0.023	0.056	-0.115
MTCI_07082017	0.171	-0.026	0.155	-0.035	0.251	-0.201
MTCI_14082017	0.041	0.241	-0.205	-0.062	0.107	0.033
NDVI$\times$PH^{-1}	-0.12	0.004	0.161	-0.004	-0.383	0.096
MTCI$\times$PH^{-1}	0.034	-0.013	0.09	0.013	-0.182	0.169

Table 5.9: P-value for Pearson correlation matrix for least square means of vegetation indices and manually measured traits. Computed for cultivars given 8 kg/daa Nitrogen fertilizer.

	GY	TKW	HLW	DH	DM	PH
TKW	0.19536					
HLW	0.76935	0.5193				
DH	0.68646	0.15965	0.81716			
DM	0.28765	0.30418	0.65053	0.2906		
PH	0.04375	0.20459	0.34453	0.27735	0.02066	
NDVI_14062017	0.06835	0.02456	0.84981	0.45257	0.69019	0.28895
NDVI_19062017	0.14379	0.00974	0.64444	0.2925	0.88318	0.57155
NDVI_29062017	0.3946	0.01655	0.95245	0.41527	0.20983	0.82964
NDVI_03072017	0.65302	0.00616	0.57039	0.21944	0.51488	0.84077
NDVI_14072017	0.96069	0.03762	0.73449	0.05098	0.80383	0.95134
NDVI_17072017	0.58218	0.02782	0.55532	0.10235	0.51858	0.79087
NDVI_25072017	0.5784	0.61575	0.21554	0.46489	0.04781	0.71333
NDVI_01082017	0.51534	0.52082	0.27138	0.27773	0.8978	0.27359
NDVI_07082017	0.4984	0.29286	0.4009	0.00417	0.00316	0.41673
NDVI_14082017	0.28776	0.66855	0.58631	0.00221	0.01085	0.3566
MTCI_14062017	0.99187	0.03215	0.15712	0.01097	0.09342	0.89303
MTCI_19062017	0.34034	0.92698	0.30523	0.83492	0.99324	0.47095
MTCI_29062017	0.44655	0.22838	0.5147	0.56381	0.6463	0.04121
MTCI_03072017	0.67443	0.4629	0.30364	0.69844	0.56427	0.08877
MTCI_14072017	0.91745	0.99477	0.90996	0.47868	0.6713	0.23953
MTCI_17072017	0.51299	0.81344	0.91289	0.34494	0.42597	0.05183
MTCI_25072017	0.65863	0.37781	0.60373	0.02682	0.97988	0.94563
MTCI_01082017	0.5853	0.30853	0.61237	0.07092	0.19374	0.00753
MTCI_07082017	0.67676	0.78205	0.71663	0.99301	0.45146	0.17061
MTCI_14082017	0.44207	0.96249	0.47031	0.51538	0.61072	0.39468
NDVI$\times$PH^{-1}	0.85933	0.08946	0.79858	0.08818	0.46899	0.04153
MTCI$\times$PH^{-1}	0.93351	0.71242	0.99623	0.21257	0.77998	0.06276

Table 5.10: Pearson correlation matrix for least square means of vegetation indices and manually measured traits. Computed for cultivars given 15 kg/daa Nitrogen fertilizer.

	GY	TKW	HLW	DH	DM	PH
TKW	0.337					
HLW	0.066	0.196				
DH	-0.023	-0.211	0.082			
DM	0.335	-0.084	-0.069	0.292		
PH	-0.363	0.315	0.228	-0.198	-0.386	
NDVI_14062017	-0.342	-0.019	0.067	-0.126	-0.26	0.127
NDVI_19062017	-0.272	0.006	0.156	-0.101	-0.203	0.107
NDVI_29062017	-0.255	-0.064	0.259	-0.14	-0.109	0.009
NDVI_03072017	-0.204	-0.118	0.149	-0.133	-0.147	-0.028
NDVI_14072017	-0.122	-0.131	0.06	-0.164	-0.077	-0.022
NDVI_17072017	-0.144	-0.122	0.035	-0.129	-0.01	-0.041
NDVI_25072017	-0.163	-0.189	-0.074	-0.167	-0.008	-0.124
NDVI_01082017	-0.192	-0.115	0.067	-0.173	-0.103	-0.026
NDVI_07082017	0.108	-0.115	0.019	-0.13	-0.024	-0.033
NDVI_14082017	0.12	-0.091	-0.017	-0.102	-0.069	-0.036
MTCI_14062017	-0.057	-0.119	0.047	-0.164	-0.101	0.004
MTCI_29062017	-0.005	-0.133	0.159	0.101	0.005	-0.001
MTCI_03072017	-0.016	-0.175	0.134	0.025	-0.003	0.002
MTCI_14072017	-0.001	-0.187	0.088	-0.071	-0.06	-0.011
MTCI_17072017	0.05	-0.171	0.063	-0.035	0.001	-0.1
MTCI_25072017	-0.106	-0.238	0.041	-0.107	-0.098	0.019
MTCI_01082017	0.081	-0.088	0.092	-0.037	-0.052	0.004
MTCI_07082017	0.015	-0.197	0.041	0.012	-0.276	-0.043
MTCI_14082017	0.154	0.096	-0.315	0.395	0.189	-0.227
NDVI$\times$PH^{-1}	-0.044	-0.079	-0.247	0.246	0.098	0.11
MTCI$\times$PH^{-1}	0.207	0.081	-0.089	0.084	0.061	0.089

Table 5.11: P-value for Pearson correlation matrix for least square means of vegetation indices and manually measured traits. Computed for cultivars given 15 kg/daa Nitrogen fertilizer.

	GY	TKW	HLW	DH	DM	PH
TKW	0.19536					
HLW	0.76935	0.5193				
DH	0.68646	0.15965	0.81716			
DM	0.28765	0.30418	0.65053	0.2906		
PH	0.04375	0.20459	0.34453	0.27735	0.02066	
NDVI_14062017	0.06835	0.02456	0.84981	0.45257	0.69019	0.28895
NDVI_19062017	0.14379	0.00974	0.64444	0.2925	0.88318	0.57155
NDVI_29062017	0.3946	0.01655	0.95245	0.41527	0.20983	0.82964
NDVI_03072017	0.65302	0.00616	0.57039	0.21944	0.51488	0.84077
NDVI_14072017	0.96069	0.03762	0.73449	0.05098	0.80383	0.95134
NDVI_17072017	0.58218	0.02782	0.55532	0.10235	0.51858	0.79087
NDVI_25072017	0.5784	0.61575	0.21554	0.46489	0.04781	0.71333
NDVI_01082017	0.51534	0.52082	0.27138	0.27773	0.8978	0.27359
NDVI_07082017	0.4984	0.29286	0.4009	0.00417	0.00316	0.41673
NDVI_14082017	0.28776	0.66855	0.58631	0.00221	0.01085	0.3566
MTCI_14062017	0.99187	0.03215	0.15712	0.01097	0.09342	0.89303
MTCI_19062017	0.34034	0.92698	0.30523	0.83492	0.99324	0.47095
MTCI_29062017	0.44655	0.22838	0.5147	0.56381	0.6463	0.04121
MTCI_03072017	0.67443	0.4629	0.30364	0.69844	0.56427	0.08877
MTCI_14072017	0.91745	0.99477	0.90996	0.47868	0.6713	0.23953
MTCI_17072017	0.51299	0.81344	0.91289	0.34494	0.42597	0.05183
MTCI_25072017	0.65863	0.37781	0.60373	0.02682	0.97988	0.94563
MTCI_01082017	0.5853	0.30853	0.61237	0.07092	0.19374	0.00753
MTCI_07082017	0.67676	0.78205	0.71663	0.99301	0.45146	0.17061
MTCI_14082017	0.44207	0.96249	0.47031	0.51538	0.61072	0.39468
NDVI$\times$PH^{-1}	0.85933	0.08946	0.79858	0.08818	0.46899	0.04153
MTCI$\times$PH^{-1}	0.93351	0.71242	0.99623	0.21257	0.77998	0.06276

Table 5.12: P-value for Pearson correlation matrix for least square means of vegetation indices and manually measured traits. Computed for cultivars only.

	GY	TKW	HLW	DH	DM	PH
TKW	0.19536	TKW				
HLW	0.76935	0.5193	HLW			
DH	0.68646	0.15965	0.81716	DH		
DM	0.28765	0.30418	0.65053	0.2906	DM	
PH	0.04375	0.20459	0.34453	0.27735	0.02066	PH
NDVI_14062017	0.06835	0.02456	0.84981	0.45257	0.69019	0.28895
NDVI_19062017	0.14379	0.00974	0.64444	0.2925	0.88318	0.57155
NDVI_29062017	0.3946	0.01655	0.95245	0.41527	0.20983	0.82964
NDVI_03072017	0.65302	0.00616	0.57039	0.21944	0.51488	0.84077
NDVI_14072017	0.96069	0.03762	0.73449	0.05098	0.80383	0.95134
NDVI_17072017	0.58218	0.02782	0.55532	0.10235	0.51858	0.79087
NDVI_25072017	0.5784	0.61575	0.21554	0.46489	0.04781	0.71333
NDVI_01082017	0.51534	0.52082	0.27138	0.27773	0.8978	0.27359
NDVI_07082017	0.4984	0.29286	0.4009	0.00417	0.00316	0.41673
NDVI_14082017	0.28776	0.66855	0.58631	0.00221	0.01085	0.3566
MTCI_14062017	0.99187	0.03215	0.15712	0.01097	0.09342	0.89303
MTCI_19062017	0.34034	0.92698	0.30523	0.83492	0.99324	0.47095
MTCI_29062017	0.44655	0.22838	0.5147	0.56381	0.6463	0.04121
MTCI_03072017	0.67443	0.4629	0.30364	0.69844	0.56427	0.08877
MTCI_14072017	0.91745	0.99477	0.90996	0.47868	0.6713	0.23953
MTCI_17072017	0.51299	0.81344	0.91289	0.34494	0.42597	0.05183
MTCI_25072017	0.65863	0.37781	0.60373	0.02682	0.97988	0.94563
MTCI_01082017	0.5853	0.30853	0.61237	0.07092	0.19374	0.00753
MTCI_07082017	0.67676	0.78205	0.71663	0.99301	0.45146	0.17061
MTCI_14082017	0.44207	0.96249	0.47031	0.51538	0.61072	0.39468
NDVI$\times$PH^{-1}	0.85933	0.08946	0.79858	0.08818	0.46899	0.04153
MTCI$\times$PH^{-1}	0.93351	0.71242	0.99623	0.21257	0.77998	0.06276

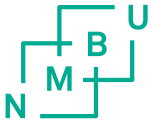

Norges miljø- og biovitenskapelige universitet
Noregs miljø- og biovitskapelege universitet
Norwegian University of Life Sciences

Postboks 5003
NO-1432 Ås
Norway